PARTICLE SEPARATOR FOR IMPROVED FLAMELESS PRESSURIZED OXY-COMBUSTION

Final Scientific Report

Award Number: DE - FE0031549
SwRI® Project No. 18.23524

Principal Investigator:
Joshua Schmitt
(PI Contact: joshua.schmitt@swri.org / 210-522-6777)

Co-Authors:
Seth Cunningham
Walter Langford
Satoshi Atsuchi
Jose Marasigan

Federal Agency to which the report is submitted:

U.S. Department of Energy (DOE)
National Energy Technology Laboratory (NETL), Pittsburgh, PA

Date of the Report:
March 31, 2023

Prime Recipient's DUNS Number: 00-793-6842

SOUTHWEST RESEARCH INSTITUTE®
6220 Culebra Road
San Antonio, Texas 78238

PARTICLE SEPARATOR FOR IMPROVED FLAMELESS PRESSURIZED OXY-COMBUSTION

Final Scientific Report

Award Number: DE - FE0031549
SwRI® Project No. 18.23524

Principal Investigator:
Joshua Schmitt
(PI Contact: joshua.schmitt@swri.org / 210-522-6777)

Co-Authors:
Seth Cunningham
Walter Langford
Satoshi Atsuchi
Jose Marasigan

Federal Agency to which the report is submitted:

U.S. Department of Energy (DOE)
National Energy Technology Laboratory (NETL), Pittsburgh, PA

Date of the Report:
March 31, 2023

Prime Recipient's DUNS Number: 00-793-6842

Approved:

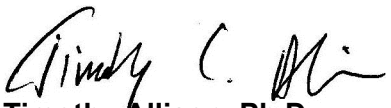

Timothy Allison, Ph.D.
Director-R&D
Machinery Department

DISCLAIMER

This report was prepared as an account of work sponsored by an agency of the United States Government. Neither the United States Government nor any agency thereof, nor any of their employees, makes any warranty, express or implied, or assumes any legal liability or responsibility for the accuracy, completeness, or usefulness of any information, apparatus, product, or process disclosed, or represents that its use would not infringe privately owned rights. Reference herein to any specific commercial product, process, or service by trade name, trademark, manufacturer, or otherwise does not necessarily constitute or imply its endorsement, recommendation, or favoring by the United States Government or any agency thereof. The views and opinions of authors expressed herein do not necessarily state or reflect those of the United States Government or any agency thereof.

TABLE OF CONTENTS

Section **Page**

LIST OF FIGURES

Figure **Page**

LIST OF TABLES

Table **Page**

1. INTRODUCTION

The team of Southwest Research Institute® (SwRI®), ITEA, Electric Power Research Institute, Inc. (EPRI), and General Electric Global Research (GE) is advancing Flameless Pressurized Oxy-combustion (FPO), a novel coal technology. This effort seeks to develop a particle separator for the hot-gas stream leaving the FPO loop. In order to maximize the energy extracted from the cycle, the hot gas is put through a turbo-expander before flue-gas treatment.

The particle separator designed under this project sought to operate at high temperature and with low-pressure drop, protecting the turbo-expander from erosion damage. The team engaged potential vendors for the test, developed plans for the pilot test loop modification, and refined requirements for the commercial turbo-expander.

2. ASSESSMENT AND SELECTION OF PARTICLE SEPARATOR TECHNOLOGY

A variety of technologies were cataloged and assessed for potential selection as the final design for the test. Once the design is selected, a test plan was developed to target key figures of merit to validate the technology. This task includes an evaluation of the future market opportunities and impacts of test results.

2.1 REVIEW AND SELECTION OF EXISTING PARTICLE SEPARATOR TECHNOLOGY

2.1.1 REVIEW OF PARTICULATE REMOVAL CONSIDERATIONS FOR GAS TURBINE EXPANDERS

The team conducted a preliminary review of particulate removal considerations for gas turbine expanders. Gas containing particulate matter can severely impact the turbine blades and internal components of a downstream turbo-expander. Of particular concern are the effects of erosion and particle deposition, which can impact the aerodynamic performance and rotordynamics of the turbo-expander. Depending on the chemical composition of the particulate matter, corrosion can also be a concern. A large body of work is available in the study of turbine blade erosion, corrosion, and deposition in gas turbines due to ingested particulate matter. Much of this work is in the study of helicopter and ground tracked-vehicle gas turbine power plants due to dust ingestion. Less work has been performed in regards to turbo-expanders for industrial or power generation use.

Damage due to particulates in the gas stream is dependent on a number of factors, including particle size, velocity, gas temperature, and particulate loading. In general, particles greater than approximately 2 μm in diameter can cause significant damage in turbo-expanders [1]. Wright and Stringer studied the high-temperature erosion and corrosion considerations for pressurized fluidized bed combustion (PFBC) gas turbine expanders (Figure 1). Smaller particles may cause less damage in proportion to the particulate load; however, there is significantly less research in regards to tolerance of fine particles by gas turbines. In addition, there is little work regarding tolerance of a particulate load from FPO combustion.

Engineering compromises may be necessary to balance the lifetime of the turbine with the degree of gas cleanup that is economical. In the consideration of separator technologies for a demonstration with FPO, it is necessary to work closely with turbine manufacturers to determine the acceptable particulate load based on the degree of gas cleanup that can be achieved and the desired turbine life.

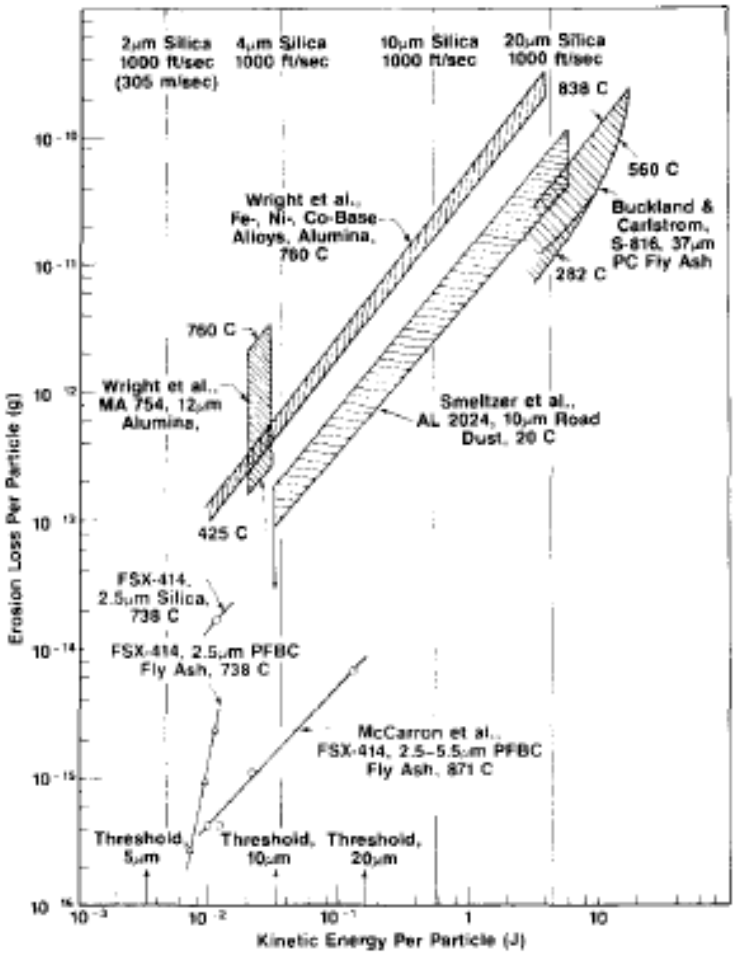

Figure 1. High-Temperature Erosion Kinetics of Some Gas-Turbine Alloys [1]

2.1.2 REVIEW OF ANALOG APPLICATIONS REQUIRING HIGH-TEMPERATURE, HIGH-PRESSURE PARTICULATE REMOVAL

The team reviewed existing particle separator technologies with special focus on analog applications that require particulate removal in high-temperature, high-pressure environments. These analog technologies are useful to gain an understanding of the requirements and challenges associated with particulate gas cleanup for FPO. Identified potential analog technologies include PFBC, coal gasification, direct coal-fired gas turbines, and metallurgical furnaces. Parker and Calvert summarize the technologies above and describe typical separation schemes in Table 1 [2]. Although not typically high temperature and pressure, particulate removal on gas turbine power plants for aero and ground-based applications are another potential analog technology due to typical reliance on momentum separators that can be scaled to high-temperature use.

Table 1. High Temperature and Pressure Particulate Cleanup Requirements [2]

PROCESS	ALLOWABLE PARTICULATE LOADING		DETERMINING FACTOR	CONTROL DEVICE USED OR PROPOSED
	S.I. UNITS	ENGLISH UNITS		
Open cycle coal-fired gas turbine, Pressurized fluidized bed coal combustion, and Combined cycle low-BTU coal gasification	2.3 mg/m³ >2 µm 43 ng/MJ <2 µm	0.001 gr/SCF >2 µm 0.1 lb/10⁶BTU* <2 µm	Turbine wear Emissions	Cyclones, followed by filters; hot electrostatic precipitators, or granular bed filters
High BTU coal gasification	4.6 mg/m³	0.002 gr/SCF	Pipeline quality	Cyclones followed by high efficiency scrubbers
FCC catalyst regenerator	0.001 gram of particulate per gram of coke burnt off	0.001 lb particulate per lb coke burnt off	Emissions	Electrostatic precipitators, baghouses, scrubbers, granular bed filters
Metallurgical furnaces (in general) Steel electric arc furnaces	50.4 mg/m³ 11.9 mg/m³	0.022 gr/SCF 0.0052 gr/SCF	Emissions Emissions	Electrostatic precipitators, high efficiency scrubbers, and baghouses

*Current new source performance standards are 0.1 lb/10⁶BTU, however a stricter standard of 0.05 lb/10⁶BTU has been proposed.

2.1.3 IDENTIFICATION OF PROSPECTIVE PARTICULATE REMOVAL TECHNOLOGIES FOR THE FPO APPLICATION

A combination-cyclone separator and tertiary filter, as shown in Figure 2, have been studied for combined-cycle PFBC power generation applications [2]. Conventional scrubber designs are generally not well suited for the tertiary-collection stage before expansion through a gas turbine due to significant temperature losses. High-temperature granular-bed filters and electrostatic precipitators have the potential for use as tertiary filters but have not been demonstrated with adequate efficiency. Non-traditional use of venture- or orifice-type scrubbers in combination with a feedwater heater to minimize temperature losses may also be possible.

While cyclone separators have long been used for high-temperature particle separation, traditional “baghouse” fabric filtration systems have not been applicable to the high temperatures. Advances in ceramic fibers for high-temperature gas filtration provide an opportunity to apply this technology to FPO gas filtration. First, et al. have demonstrated the application of *Fiberfrax* ceramic elements for filtration of small particulate matter from gases at temperatures above 1,000°F [3]. A high-temperature filter bag has been demonstrated at the 5-MWe scale as part of the Babcock & Wilcox Company’s SOx-NOx-Rox Box™ process [4].

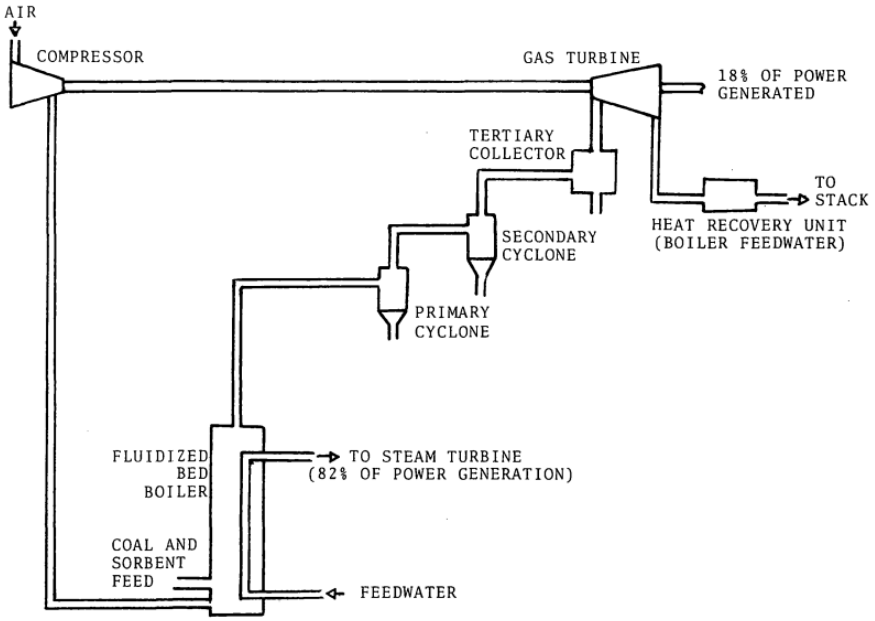

Figure 2. Combination Cyclone Separator and Filter for Combined-cycle PFBC Power Plant [2]

Momentum separator designs have successfully been used for particulate separation in gas turbine power plants for aero- and ground-based applications. Many of these designs are scalable to high-temperature high-pressure applications with consideration to the material properties. One such design is a curvature separator developed by GE presented in Figure 3.

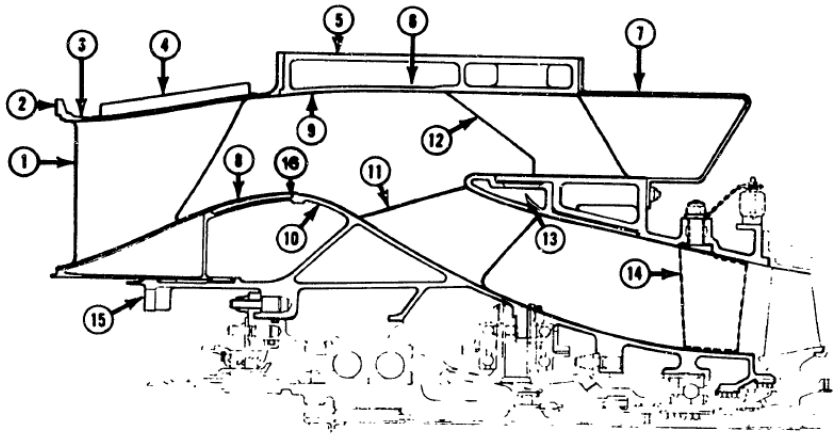

1. INLET SWIRL VANE
2. FORWARD QUICK-DISCONNECT FLANGE CUSTOMER CONNECTION
3. SWIRL FRAME
4. ANTI-ICING MANIFOLD
5. MAIN FRAME
6. OIL TANK
7. SCAVENGE AIR COLLECTOR
8. INNER WALL
9. OUTER WALL
10. FRONT FRAME
11. DESWIRL VANE
12. SCAVENGE AIR VANE
13. ANTI-ICING AIR PLENUM
14. COMPRESSOR INLET GUIDE VANE
15. CUSTOMER CONNECTION
16. RAINSTEP

Figure 3. Design for a Curvature Particle Separator [5]

The project team worked to review and identify prospective technologies that could be used for particulate separation in FPO applications with high temperature, high pressure, and low-pressure drop requirements.

2.1.4 FPO Flue Gas Conditions Entering the Separator

This project's chosen separator test site was the existing FPO 5-MWth pilot facility in Gioia del Colle, Italy. A simplified block diagram of the commercialized FPO process is shown in Figure 4. The intended location of the separator is immediately following the turbo expander quencher. Depending on the temperature performance of the designed separator, colder regions of the FPO loop may be considered for additional particle removal.

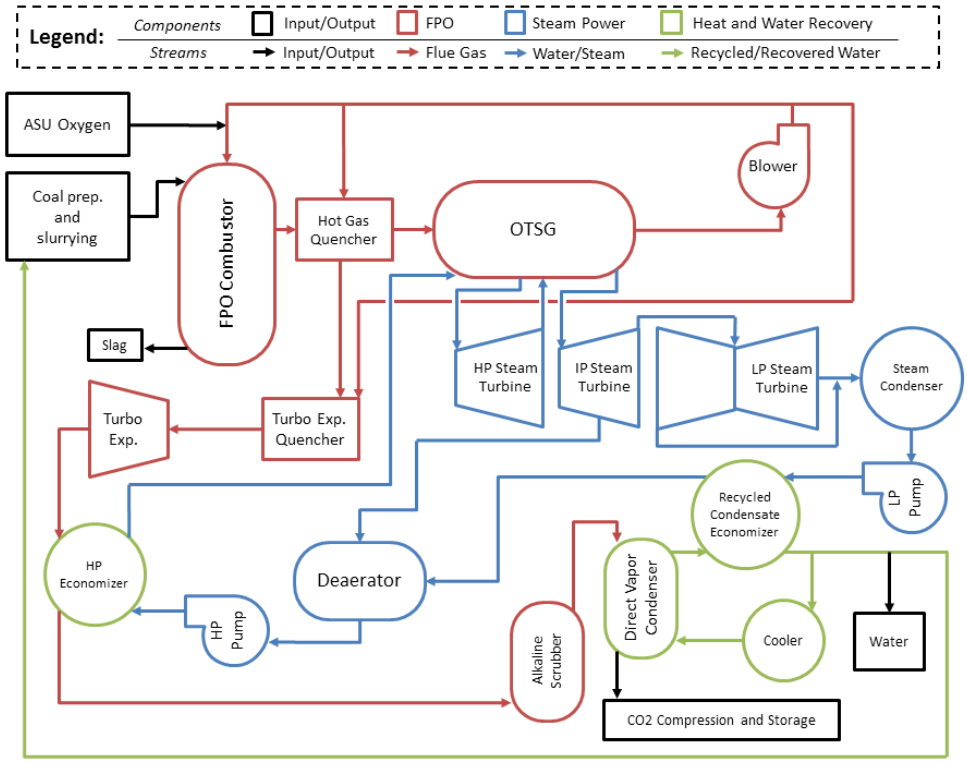

Figure 4. Block Diagram of the Commercial FPO Cycle

Historical data from a variety of feedstocks have been taken on at the 5-MWth facility. A sample of the particle distributions from a run at the facility is shown in Figure 5..

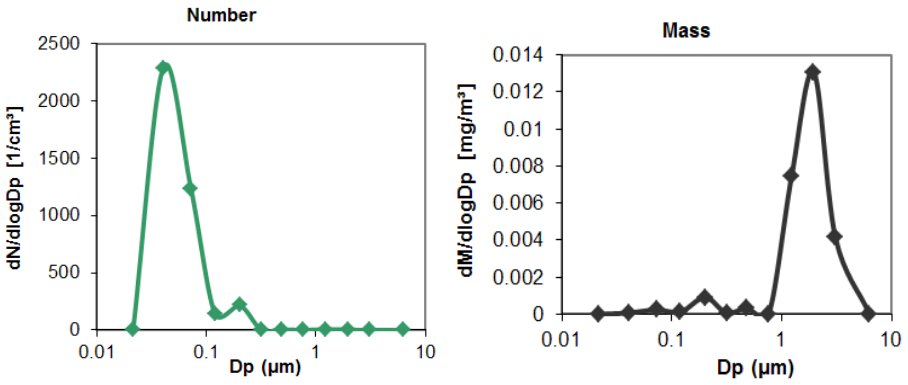

Figure 5. Distribution of Particulate Measured from FPO 5-MWth Testing

The flue gas drag force, which is dependent on the density, is one key factor to match for particle separation. Turbo-expander inlet flue gas density in a commercial-scale FPO cycle is approximately 3.68 kg/m^3. The 5-MWth pilot can achieve 3.45 kg/m^3 density gas with a volumetric flow rate from 0.13 m^3/s to 0.27 m^3/s at the boiler exit.

2.2 EVALUATION OF CANDIDATE TECHNOLOGIES

2.2.1 INERTIA SEPARATOR

One candidate is the inertia separator, as shown in Figure 6. This is a compact technology with no moving parts that can be done in multiple configurations. In addition, the pressure drop is potentially very low. It is efficient for large particles above 10 µm but struggles below that size. Inertia separators also require a scavenge flow which could severely impact cycle performance.

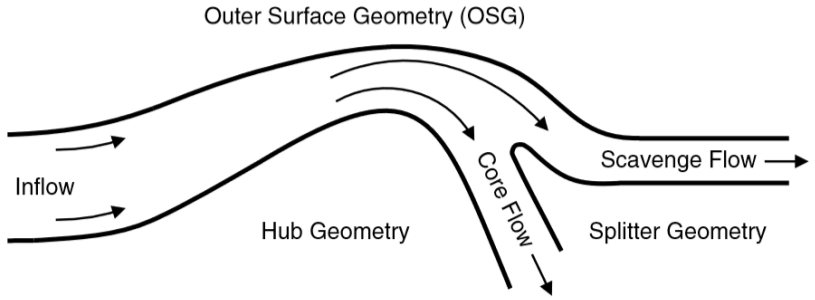

Figure 6. Cross Section Schematic of an Inertia Particle Separator

2.2.2 CYCLONE SEPARATOR

Figure 7 shows the basic principles behind a cyclonic separator. The high curvature of flow is effective, even below 10 µm; however, below 1 µm, the efficiency can be approximately 50%. The technology is compact with no moving parts and can maintain a low-pressure drop. Erosion is a potential concern, and there is a scavenge flow that can impact cycle efficiency.

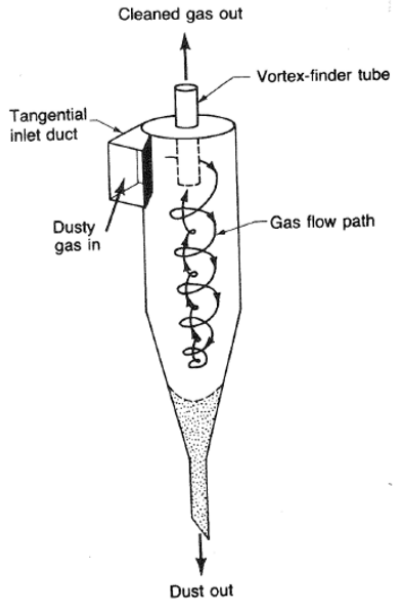

Figure 7. Schematic Diagram of a Cyclone Separator

2.2.3 ACOUSTIC AGGLOMERATOR

Acoustic agglomeration, demonstrated in Figure 8, can cause smaller diameter particles to stick together and form effectively larger particles. The large particles can then be separated through other means at reduced pressure drop requirements, depending on the separator technology that it is paired with. This technology is not yet commercially available, but it has shown promising results in lab tests. It also comes with a power requirement.

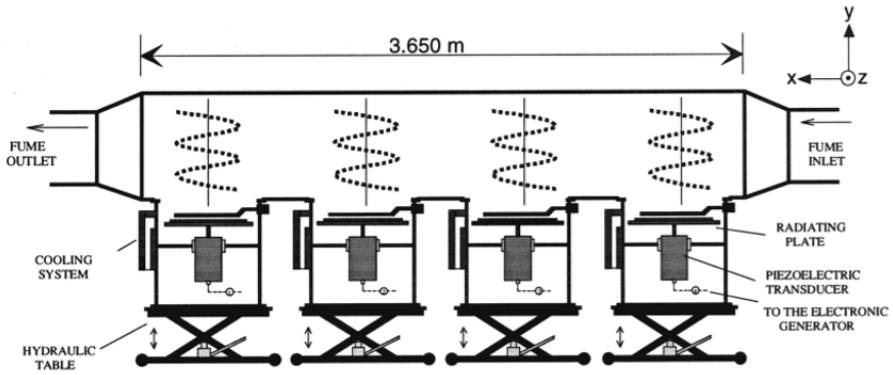

Figure 8. Schematic Diagram of Acoustic Agglomeration

2.2.4 BAGHOUSES AND BARRIER FILTERS

Baghouses and barrier filters, represented in Figure 9, are common and conventional means for removing coal ash particulate. They are capable of collecting 99.9% of particles. A ceramic material would be required for high-temperature applications. They do require regular cleaning and particle removal to be effective. They also can have a high-pressure drop depending on the required diameter of particle removal. One further potential detractor is a large amount of space generally required to house a baghouse or barrier filter.

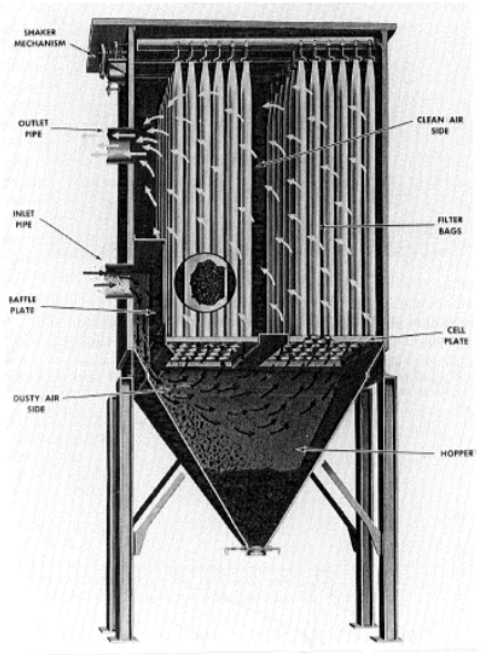

Figure 9. Diagram of a Bag House or Barrier Filter

2.2.5 ELECTROSTATIC PACKED GRANULAR BED FILTER

Figure 10 outlines the concept behind an electrostatic packed granular bed filter. This filter uses electrostatic charging of the particles and is capable of removing very small particles. Depending on the packing of the bed, the pressure drop can be low, but removal efficiency may suffer. The technology is also not very far in commercial development and may require extensive testing to be ready for commercialization. As particulate is removed, the bed must be refreshed, which can be done continuously or in batches.

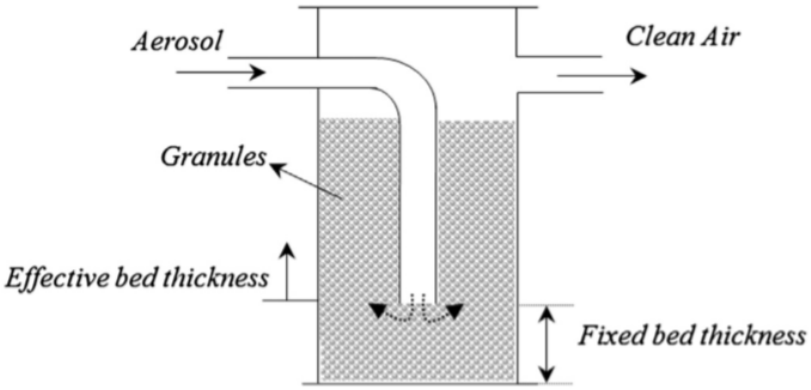

Figure 10. Diagram of an Electrostatic Granular Bed Filter

2.2.6 VENTURI SCRUBBER

Figure 11 demonstrates the concept behind a venturi scrubber. Water is injected into the system, and the condensed droplets trap small particles effectively. However, water will not be liquid at expected turbo-expander temperatures, so this technology is not likely to pair well with FPO.

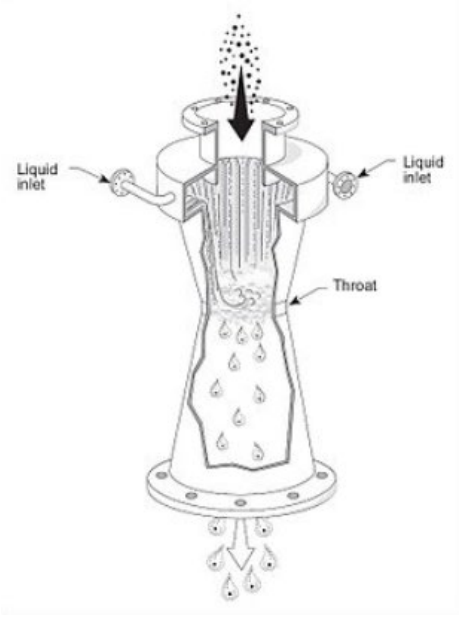

Figure 11. Schematic Diagram of a Venturi Scrubber

Electrostatic particle separation could be paired with some of the above technologies allowing for an attraction and removal of finer particles. It is not fully compatible with every technology and should be considered carefully depending on particle removal needs.

Chemical agglomeration, similar to acoustic agglomeration, could be used with other separation technologies to effectively remove fine particles. The chemical compatibility of the separator with the required chemicals is the primary concern.

2.2.7 ELECTROSTATIC PRECIPITATOR

Figure 12 shows a cut-away of an electrostatic precipitator. The technology readiness level (TRL) of this separator is high for common commercial applications. Pressure drop can be managed, and the separation efficiency can be high for small particle removal. The negative aspects of this technology include its large size, its parasitic power requirement, and its cleaning and maintenance requirements.

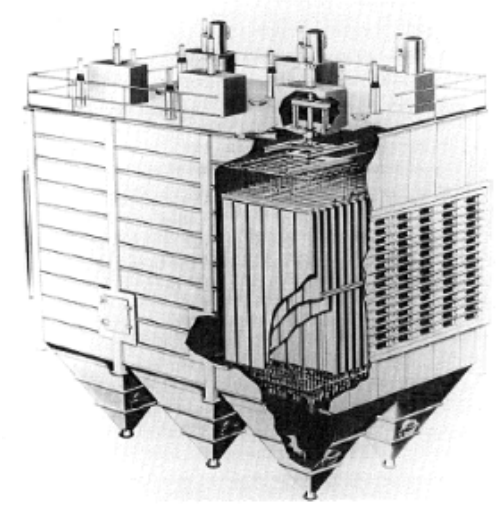

Figure 12. Diagram of an Electrostatic Precipitator

2.3 CRITERIA FOR RATING CANDIDATE TECHNOLOGIES

The team compiled a set of evaluation questions for the candidate technologies as shown in Table 2. The table also includes a weighting factor that was developed for each criteria.

Table 2. Evaluation Criteria and Weighting for Assessing Technologies

Program Goals	Weighting
Is the technology scalable? (5-MW demonstration, 50-MW Pilot, Utility Scale)	**High**
Does the technology have applicability to other systems/industries?	**Low**
Is the technology of commercial interest to the participating organizations?	**Low**
Is the technology of commercial interest to any other industries?	**Medium**
Is the technology of interest to the scientific community? (i.e., advance the state-of-the-art)	**Low**
Physical Attributes	
Are there little or no special permits required to operate the equipment?	**High**
Are there little or no corrosion concerns with the equipment/system?	**Medium**
Are little or no special materials/manufacturing processes required?	**Medium**
Is the equipment/system not sensitive to different types of coal flue ash?	**Medium**
What is the compactness of the equipment/system?	**High**
Does the equipment/system operate independently from other systems?	**Medium**

Does the equipment require little or no support system or specialized equipment?	**Medium**
Operations	
How do changes in temperature/pressure/gas flow affect the system efficiency?	**High**
Does the system require pneumatics/hydraulics?	**Medium**
Does the system require power?	**Medium**
Does the system effectively remove particles above 1 µm in diameter?	**High**
Does the system effectively remove particles between 1 µm-0.4 µm in diameter?	**High**
Does the system effectively remove particles below 0.4 µm in diameter?	**Medium**
Can the system/equipment be located outside without cover or protection?	**Medium**
Are there little or no the system maintenance requirements?	**High**
Is the separator pressure drop less than 4%?	**High**
Is the separator pressure drop less than 2%?	**Medium**
Is the equipment/system capable of 24/7 operation?	**High**
Is the system tolerant to high temperatures up to 500°C?	**High**
Is the system tolerant to high temperatures (500-700°C)?	**High**
How reliable is the system?	**High**
Is there a long expected service life?	**Medium**
Does the startup/commissioning procedure have little or no impact on plant procedure?	**Medium**
Are there little or no major design/operations impacts on the rest of the cycle? (i.e., shifts in operating points, system response times, system piping dynamics/acoustics, etc.)	**High**
Does potential failure modes have little or no consequences?	**High**
Does system-monitoring requirements have little or no impact on plant cost/operation?	**High**
Environmental and Permitting	
Are waste products generated safe?	**Medium**
Is the equipment safe while operating?	**High**
How quiet is the equipment?	**Medium**
Is there low permitting risk? (i.e., Potentially changing standards, no defined standards, etc.)	**Medium**
Are there little or no emissions from the equipment/system?	**Medium**
Business and Financing	
Is the equipment/system at a TRL above 6?	**Medium**
Does the equipment/system have a short lead-time?	**High**
Is there low acquisitions risk? (i.e., single supplier, exotic materials, etc.)	**Medium**
Is there a limited amount of potential import/export controls associated with technology?	**Low**
Does operation of the equipment/system require little manufacturer support for operation?	**High**
How low is the projected system/equipment cost?	**High**
Does any of the participating organizations have experience with the equipment/system?	**Medium**

2.3.1 ELIMINATION OF CANDIDATE TECHNOLOGIES

The team looked at the technologies being considered, disqualifying certain technologies based on several criteria. The potential technology needed to be compact in size and able to fit between the steam generator and the turbo-expander. The TRL needed to be above 6 due to the program goals of producing a mature system demonstration. The TRL, in this case, is demonstrated by availability of commercial products and published literature with performance and cost data. A technology was also eliminated if it had high potential for high pressure loss and low particle separation efficiency.

One final factor in the initial round of down-selection is the particle size separation required in the turbo-expander. The team evaluated expander passages and calculated the Stokes number. The Stokes number is shown in Equation 1, and it gives the size at which a particle will separate from the flow path.

Equation 1. Stokes Number

$$Stokes\ Number = \frac{\left(\rho_p {d_p}^2 / 18\mu_f\right) u_f}{l}$$

where

ρ: density
d: diameter
μ: dynamic viscosity
u: velocity
l: characteristic length

subscript:
p: particle
f: fluid

Conservative estimates indicate that particles of the diameter larger than 1 micron would separate from the flow path at the turbo-expander rotor inlet. Thus, separation efficiencies should be high for particles above that diameter.

The acoustic agglomerator and the electrostatic granular bed filter were removed from candidacy for their low TRL and lack of supporting literature. The ceramic bag house was disqualified for scoring poorly in compactness. Finally, the venturi scrubber was eliminated for its incompatibility with the FPO high-temperature conditions.

The remaining candidate technologies are the inertia separator, cyclone, ceramic barrier filter, and electrostatic precipitator.

2.3.2 Detailed Technology Evaluation Results and Down-Selection

A detailed literature search on the remaining technologies was performed by the organizations involved in the down-selection. This led to scoring them on a 1 to 5 scale for each criterion. The weighting ranges from 1 to 3, depending on if the weight is low, medium, or high. The score for each technology is shown in Table 3. The scores were discussed as a group and adjusted as necessary. This process should help to account for any bias in the individuals generating the initial scores.

Table 3. Scoring for the Final Candidate Technologies

Program Goals	Inertia Separator	Cyclone	Ceramic Barrier Filter	Electrostatic Precipitator
Is the technology scalable? (5-MW demonstration, 50-MW Pilot, Utility Scale)	3	3	5	5
Does the technology have applicability to other systems/industries?	5	5	5	5
Is the technology of commercial interest to the participating organizations?	3	3	2	2
Is the technology of commercial interest to any other industries?	4	4	4	3
Is the technology of interest to the scientific community? (i.e., advance the state-of-the-art)	3	3	5	5
Physical Attributes				
Are there little or no special permits required to operate the equipment?	4	4	4	4
Are there little or no corrosion concerns with the equipment/system?	3	3	4	3
Are little or no special materials/manufacturing processes required?	5	5	4	5
Is the equipment/system not sensitive to different types of coal flue ash?	4	4	3	4
What is the compactness of the equipment/system?	4	3	2	2
Does the equipment/system operate independently from other systems?	4	4	3	4
Does the equipment require little or no support system or specialized equipment?	4	4	3	2
Operations				
How do changes in temperature/pressure/gas flow affect the system efficiency?	2	4	3	4
Does the system require pneumatics/hydraulics?	5	5	2	5
Does the system require power?	3	3	4	1
Does the system effectively remove particles above 1 µm in diameter?	4	4	5	3
Does the system effectively remove particles between 1 µm-0.4 µm in diameter?	2	3	4	4
Does the system effectively remove particles below 0.4 µm in diameter?	2	3	4	3
Can the system/equipment be located outside without cover or protection?	4	4	3	3
Are their little or no system maintenance requirements?	4	4	2	2
Is the separator pressure drop less than 4%?	4	4	5	5
Is the separator pressure drop less than 2%?	2	2	5	5
Is the equipment/system capable of 24/7 operation?	5	5	5	5
Is the system tolerant to high temperatures up to 500°C?	5	5	5	5
Is the system tolerant to high temperatures (500-700°C)?	5	5	5	5
How reliable is the system?	5	5	1	3
Is there a long expected service life?	5	5	2	3
Does the startup/commissioning procedure have little or no impact on plant procedure?	4	5	4	1
Are there little or no major design/operations impacts on the rest of the cycle? (i.e., shifts in operating points, system response times, system piping dynamics/acoustics, etc.)	2	5	4	2
Does potential failure modes have little or no consequences?	3	3	5	1
Does system-monitoring requirements have little or no impact on plant cost/operation?	4	4	3	1
Environmental and Permitting				
Are waste products generated safely?	1	1	1	1
Is the equipment safe while operating?	4	4	4	4
How quiet is the equipment?	3	2	4	4
Is there low permitting risk? (i.e., potentially changing standards, no defined standards, etc.)	4	4	4	4
Are there little or no emissions from the equipment/system?	5	5	5	5
Business and Financing				
Is the equipment/system at a high TRL?	3	4	4	3
Does the equipment/system have a short lead-time?	3	3	3	3
Is there low acquisitions risk? (i.e., single supplier, exotic materials, etc.)	4	4	4	3
Is there a limited amount of potential import/export controls associated with technology?	5	5	5	5
Does operation of the equipment/system require little manufacturer support for operation?	4	4	5	3
How low is the projected system/equipment cost?	3	3	2	1
Does any of the participating organizations have experience with the equipment/system?	4	4	1	1

The weight is multiplied by the score, and the total scores are summed. The results are represented in Table 4. The cyclone is the best candidate for application to the FPO system. The inertia separator was disqualified as a secondary option because of its lower TRL and similarity to the primary candidate. The ceramic barrier filter was eliminated due to the potential frequent clogging and maintenance cycles associated with FPO. The electrostatic precipitator was removed from candidacy due to the technical risk associated with electrostatic equipment in a high-temperature environment. The cyclone was then assessed for design, sizing, performance, integration into the test site, and preliminary design of package.

Table 4. Total Scores by Category for the Final Candidate Technologies

Category	Inertia Separator	Cyclone	Ceramic Barrier Filter	Electrostatic Precipitator
Program Goals	31	31	36	36
Physical Attributes	64	61	52	54
Operations	166	188	164	137
Environmental and Permitting	38	36	40	40
Business and Financing	57	59	53	40
Total	356	375	345	307

2.4 EVALUATE FUTURE MARKET OPPORTUNITIES

With the selection of the cyclone separator as the particle separation technology to be tested at the test facility and to be used for commercial applications based on successful testing, the project team has outlined a preliminary plan to evaluate the future market opportunities for the separator technology. These opportunities extend to other applications beyond the ITEA FPO system.

For the cyclone technology, the team began an assessment of the economic potential of the separator and appraised its utilization for power generation applications and other coal processes beyond FPO. For the FPO combustion system as a whole, a U.S. market assessment looks at existing plants that might be suitable for repower application, opportunities for new build, and future opportunities for CO_2 such as carbon capture, utilization, and geologic storage (CCUS) as well as enhanced oil recovery. For the international market assessment, the team began identifying favorable conditions that consider fuel prices, market needs, regulations, CO_2 pricing, CCUS opportunities, need for water, and national interest in coal and CO_2 reductions.

In addition to the ITEA FPO system, power generation applications that require fly ash removal from hot gas have been identified including pulverized coal, integrated gasification combined cycle, and pressurized fluidized bed combustion. For each application, the existing methods of fly ash removal are being reviewed, and an assessment of where the cyclone separator technology can be utilized is being made either as the primary particulate removal device or as a pre-filter. Areas where the cyclone separator technology may provide an advantage (e.g., lower pressure drop resulting in improved process performance) were noted.

The evaluation also includes a high-level assessment of the FPO combustion system as a whole for the U.S. as well as international market opportunities.

2.4.1 EXPECTED PERFORMANCE FOR A LARGE-SCALE TURBO-EXPANDER

As part of the FPO scale-up analysis, a turbo-expander sized for a 25 MWth combustor loop was used. The nominal power output would be 975 kW of shaft power. This turbo-expander design

corresponds to a 11,000 rpm with 14 stages of expansion and 14,400 kg/h of flue gas flow. The inlet temperature and pressure are 520°C and 12.2 bara, respectively. The outlet temperature and pressure are 340°C and 2.47 bara, respectively. This design is expected to be maintained for a full-size expander, which would be approximately 7 to 6 MWe of output power

2.4.2 AIRFOIL EROSION PREVENTION

The first stage stator is designed with Inconel 718 as the airfoil material. This is to withstand high-temperature inlet conditions. The particulate is not expected to impact these surfaces, so no coating is applied to these airfoils. The first stage rotor is specified as a stainless steel (x22CrMoV12.1) with a coating of Chromium Carbide (CrC) to provide erosion protection. This airfoil metal and coating specification is maintained for stages 2 and 3. None of the remaining 11 stages include the erosion protection coating. This indicates that mitigating efforts can be implemented in the turbo-expander to allow the machinery to survive in a particle-loaded environment without a separator. However, even if the turbo-expander can survive in the flue gas without a particle separator, the current particle loading may result in higher costs that could impact the expected low cost of electricity of FPO.

These coatings and materials may be expensive to include in the commercial turbo-expander. The primary concerns that would add cost to the FPO system would be high initial costs, short maintenance cycles, and frequent part replacements. The removal of large particles reduces erosion events. In addition, the removal of fine particles in the 2-10 μm diameter range will also reduce the loading on the turbo-expander airfoils and increase part life. As part of the commercial analysis, the team examinrf the choice of materials, project costs, and other improvements provided by a particle separator.

3. DESIGN OF THE PARTICLE SEPARATOR

The team looked at potential configurations that integrate with the FPO cycle. Selection of the separator technology shifted to a ceramic candle filter.

3.1 FLOW ANALYSIS CRITERIA

In order for the proposed FPO power plant to provide the intended service life, the addition of a particle separator device is strongly desired to remove the harmful flue gas particulates upstream of the turbo-expander. An effective separator will mitigate erosion concerns for the turbo-expander and its downstream components by removing those damaging particles. However, too stringent separator performance requirements will negatively impact the efficiency and cost of the plant. Therefore, it is important to rationally assess the target specifications of the separator. Specifically, in this study, the required separation capability with regards to particle size is investigated and determined.

The team calculated a “cut-off” particle size criterion with sensitivity analysis, which helps guide the desired separator performance specification and down-select process. GE draws from its technical expertise in sand separator R&D for turbomachinery applications to create a specification that adequately protects the turbo-expander.

It is noted that the current studies are conducted under a 0-D/1-D assumption where no space-resolved analyses are performed for a system-level plant design purpose.

3.1.1 APPROACH

A non-dimensional parameter, called Stokes Number, is used to evaluate how likely it is that entrained particles in the flue gas leave streamlines and impact on the turbo-expander surfaces, causing erosion. The Stokes Number is defined in Equation 1.

The Stokes Number indicates how well a particle moves along a local flow streamline within a suspending fluid. When the Stokes Number is small (<<1) particles tend to follow a local streamline. Contrary, if the Stokes Number is large (>>1) particles travel like a ballistic object, and their trajectory crosses flow streamlines.

In this study, the airfoil leading edge region of the turbo-expander is the area that is most prone to erosion by the particulate impacts. Figure 13 shows a schematic of notional particle trajectories under a typical flow field around an airfoil leading edge. The grey lines represent flow streamlines. The left-hand image illustrates a case where the particle Stokes Number is small; a particle behaves as if “massless” and travels along a flow streamline. Under this condition, the particle would go around the leading edge and would not impact on the airfoil. Conversely, when the particle Stokes Number is much larger than 1, as shown in the right-hand figure, a particle trajectory tends to be “straight” regardless of surrounding flow direction, and an impact would occur. The latter situation would lead the high erosion risk, and hence needs to be avoided. A Stokes Number of 0.05 is used as a threshold value which divides these two conditions based on GE’s experience. From the Turbo-expander design study described below, an estimated upstream velocity of an airfoil is used for the fluid velocity, while the leading-edge radius of an airfloil is taken as the characteristic length. Finally, the “cut-off” particle size is computed as d_p in Stokes Number definition in Equation 1.

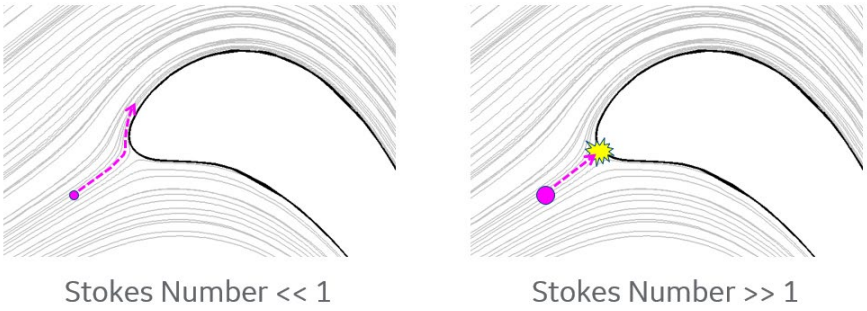

Figure 13. Typical Expected Particle Trajectories under a Representative Flow Field around an Airfoil Leading Edge

Based on the calculated "cut-off" particle size, the specification of a particle separator is determined so that any particles in the flue gas larger than the "cut-off" size are to be removed prior to the inlet of the Turbo-expander.

3.1.2 PARTICULATE ANALYSIS OF FPO FLUE GASSES

ITEA supplied additional information about the FPO flue gas particulate in the form particle size distribution from an electrical low pressure impactor (ELPI), scanning electron microscope (SEM) images, and energy-dispersive X-ray spectroscopy (EDXS) analysis of particles captured from a coal combustion test run at the 5-MWth Pilot in 2008. The ELPI data provided the distribution of particles by diameter and mass, as shown in Figure 14. The EDXS analysis in Table 5 provides particulate compositions corresponding to the samples (a), (b), (c), and (d) in the SEM images in Figure 15. The sampled compositions appear to be typical of coal fly ash. From this composition, a rough particle density range of 2.9-3.1 g/cm^3 can be estimated for particles in the 1.0 µm range assuming that such particles will be solid (i.e. non-cenospheric) and of uniform composition.

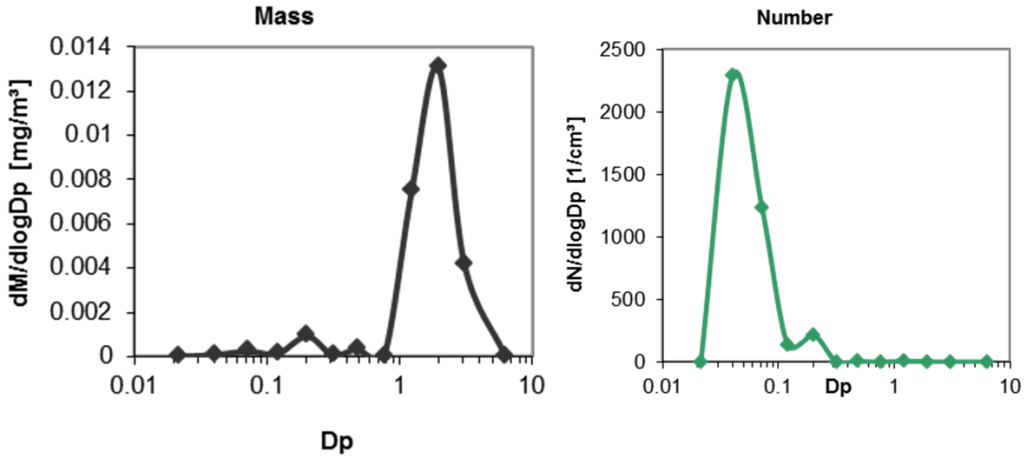

Figure 14. ELPI Particulate Analysis – ITEA 5-MWth Pilot Separator Inlet

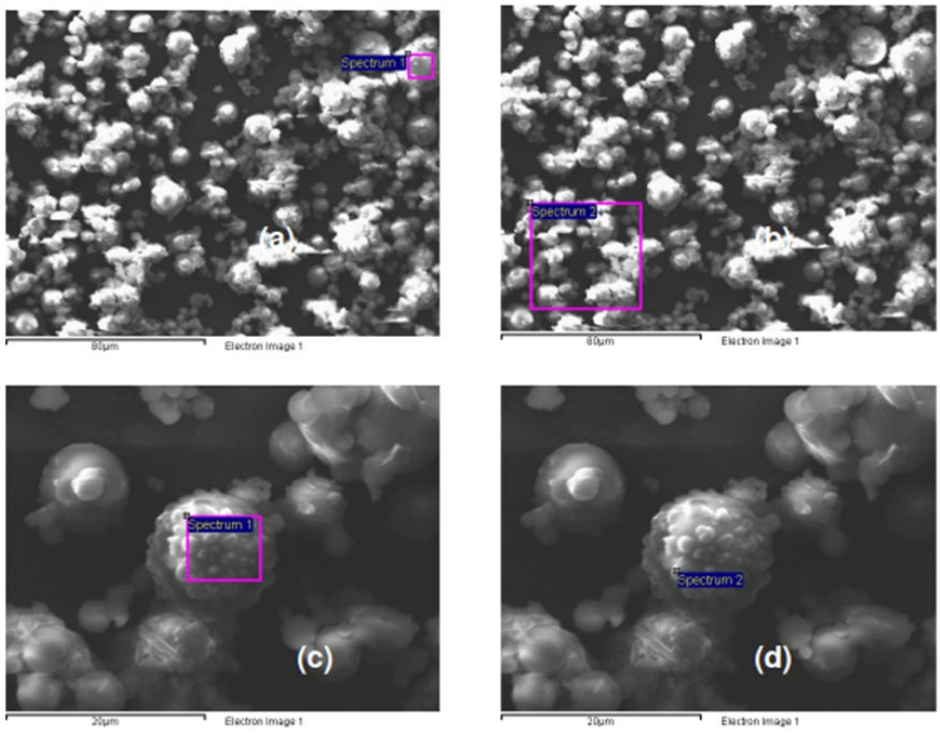

Figure 15. SEM Images of Flue Gas Particulate in the Downstream Quencher Tube

Table 5. EDXS Analysis of Flue Gas Particulate in the Downstream Quencher Tube

	a	b	c	d
	wt%	wt%	wt%	wt%
Na_2O	0.5	1.6	1.1	1.3
MgO	1.6	1.4	1.1	1.0
Al_2O_3	20.2	17.1	22.9	17.8
SiO_2	50.8	40.7	52.9	38.4
SO_3	4.2	16.6	7.6	20.7
K_2O	5.1	9.9	6.7	9.8
CaO	11.4	6.3	5.1	6.4
TiO_2	0.6	2.0	-	-
FeO	5.6	4.4	2.7	4
Cr_2O_3	-	-	-	1

Further analysis information from ITEA showed the composition of particulate for two different test campaigns. Images of an SEM analysis of particulate from a test from 2008 are shown in Figure 16. This analysis provided particle size and morphology.

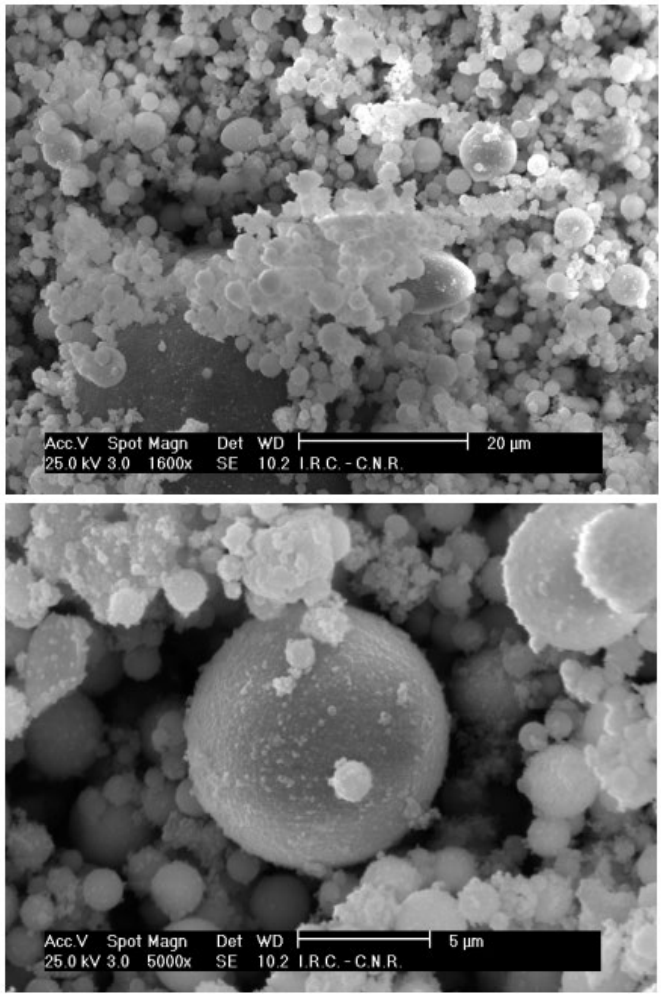

Figure 16. SEM Images of Particulate at 1,600x (Top) and 5,000x (Bottom)

Inductively coupled plasma mass spectrometry (ICP-MS) was used to evaluate the metal content of particulate collected in two trials. The results of the ICP-MS testing are shown in Table 6.

Table 6. Weight of Metals in Particulate from Two Separate Trials

	June 30, 2008	September 21, 2009
	% wt.	% wt.
Al	5.03	8.10
Ca	1.41	5.44
Fe	6.99	3.90
K	7.79	6.15
Mg	0.59	0.74
Na	1.15	1.03
Si	19.52	17.83
Ti	0.27	0.36
Total	42.75	43.55

3.1.3 PERSPECTIVE ON PARTICLE CHARACTERISTICS IN FPO

ITEA shared some of their experience on the 5-MWth pilot, which ran on a bag filter for 14 years. ITEA noticed that the absence of silico-aluminates in the fly ash was making the system very sensitive to alkaline sulfates. This was true even when present in a limited amount in the fuel. In these instances, ITEA increased the sodium carbonate upload.

Fortunately, alkaline sulfate particles are not abrasive with a low Young's modulus and very low break stress. Previous flow analysis said that when dealing with low modulus surface material and round shape, the typical hard dendritic primary particle abrasive phenomenon is not predicted to occur, even for particles much bigger than 1 µm.

These factors will need to be considered when demonstrating the type and size of particles collected in the particle removal.

3.2 TURBO-EXPANDER FLOW ANALYSIS

To estimate flow conditions around the airfoil leading edge and obtain the required input parameters in the Stokes Number, the design and architecture of a Baker Hughes, a GE Company (BHGE), and turbo-expander are utilized as a starting point. An aero "scaling" technique and GE's turbine design tools are employed to obtain viable design parameters for the proposed FPO plant turbo-expander. In addition, an exploratory study is being conducted to assess a sensitivity of the performance of the separator requirement to possible design variations of the turbo-expander.

3.2.1 FLUE GAS PROPERTIES

Because working fluid temperature changes more than 200°C through the turbo-expander based on the Aspen Plus system model prediction, temperature-dependent dynamic viscosity should be used in Stokes Number calculation as a first order effect. The flue gas viscosity is derived as a mass-weighted mixture of the composing gas viscosities. The flue gas composition at the turbo-expander inlet is predicted and presented in Table 7. Note that components with a mass fraction of less than 1% are ignored in this study.

Table 7. Predicted Flue Gas Composition at Turbo-expander Inlet for Commercial FPO System

Component	Mass Fraction
H_20	36.1%
N_2	1.0%
O_2	1.6%
AR	2.2%
CO_2	59.2%
Total	100.0%

Figure 17 shows variations of the calculated viscosity of the flue gas within a temperature range of the turbo-expander section, approximately between 700 and 1,000 K. Also plotted in Figure 17 is the viscosity of an individual component as a function of temperature [6] used for the derivation. Note that the viscosity at the atmospheric condition is used for a first order estimation and the little dependency of the viscosity on pressure.

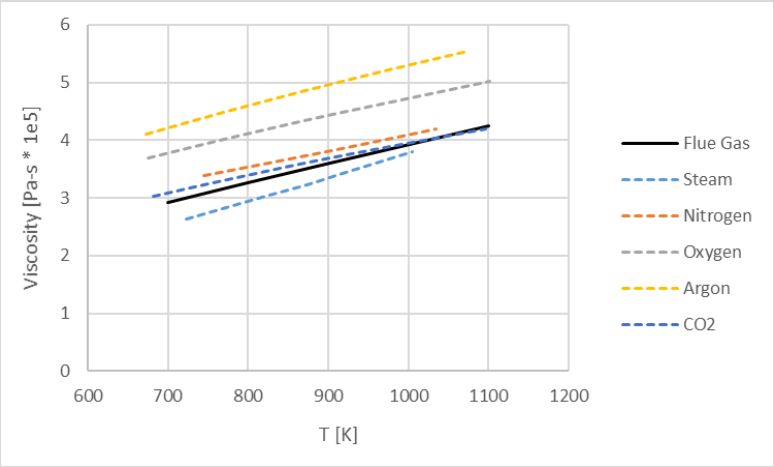

Figure 17. Gas Viscosity

While more specific data needs to be collected and analyzed, the flue gas particulate is assumed to be substantially composed of silicon with a bulk density of 1.6 g/cm^3.

3.2.2 Airfoil Aerodynamic Property Estimates for Separator Particle Size Cutoff Calculation

The pilot plant application utilizes a pre-engineered turbo-expander design produced by BHGE. The expander, shown in cross section in Figure 18, is derived from BHGE's line of modular design reaction steam turbines. While many aerodynamic properties of the turbine stages are available for the template design, the calculations required to perform particle size cut-off for separator sizing requires highly detailed, local aerodynamic information that is typically not available without detailed airfoil designs and aerodynamic through-flow models. The following sections describe the process by which the separator calculation inputs were derived from the stage data provided by BHGE.

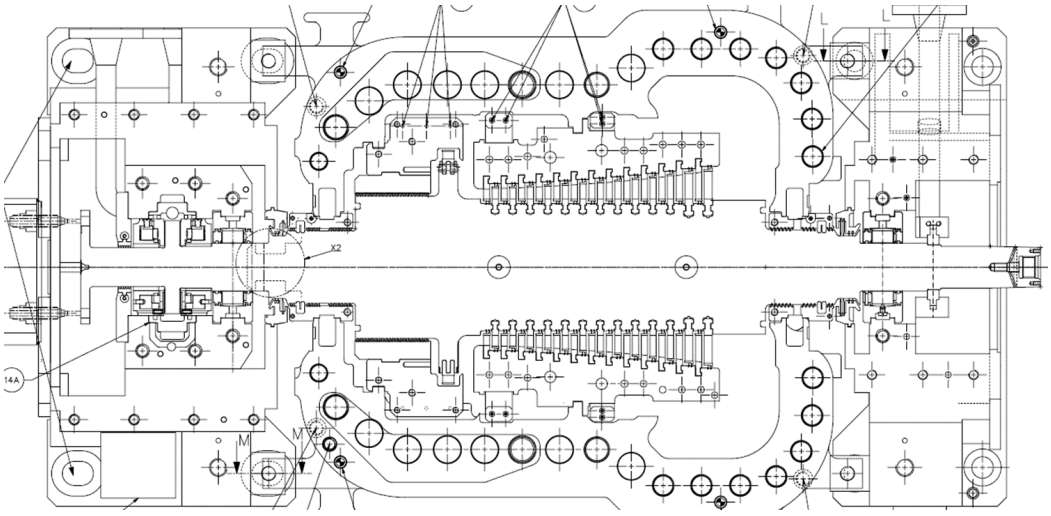

Figure 18. Representative Cross Section of Pilot Plant Turbo-expander

3.2.3 PILOT SCALE

Stage property details for the 8-stage pilot plant turbo-expander were provided to GE Global Research by BHGE. The disclosed properties are shown in Figure 4. To calculate the particle size cut-off, three additional properties not available from this data set are also required:

- Leading edge diameter of the airfoils (reference length)
- Inlet relative velocity for each airfoil (reference speed)
- Inlet static temperature for each airfoil (input to determine viscosity)

None of these properties are available from the BHGE data directly, requiring additional design estimations to complete the separator sizing calculations.

To produce the required inputs for the separator sizing calculations, an approximate detailed aerodynamic design of the pilot scale flow path was created. Using the BHGE data from Table 8, the turbine pitchline, annulus height, and velocity triangles were approximated through the following procedure:

- Gas properties were back-calculated from the BHGE data (from enthalpy and temperature) and represented simply as a gas constant and a stage-by-stage average values for specific heat (cp) and specific heat ratio (gamma).
- Stage pressure ratio (PR) was calculated from the inlet total pressure (P0) and the exit total pressure (P1) in Table 8.
- Stage exit total temperature (TTex) was calculated from PR and the efficiency reported in Table 8 (ETAI) using the ideal gas definition of total-to-total efficiency.
- Stage enthalpy drop was calculated from the change in total temperature from stage inlet to stage exit and the stage average cp. Values derived from this process were checked against the values implied directly from Table 8 (H0-H2I). The approximate ideal gas calculations were within 2% of the BHGE data in Table 8.
- Pitchline wheel speed (Up) was calculated from the work coefficient (PSI in Table 8) and the enthalpy drop, using the definition of PSI. Like enthalpy drop, the stage wheel speeds calculated with this process were checked against the values reported in Table 8 (U2). Deviations were within +/- 2% of the BHGE values.
- Pitchline diameters (Dp) for the rotor blades were calculated from Up and turbine rpm.
- Stage exit swirl angles (alpha2) were calculated from stage exit axial velocity (C2Z) and stage exit tangential velocity (C2U) from Table 8.
- Stage exit absolute velocities (C2) were calculated from flow coefficient (PHI in Table 8), alpha2, and Up using velocity triangle relationships.
- Stage exit static temperatures (TSex) were calculated from TTex, C2, and isentropic relationships.
- Stage exit Mach numbers (Mex) were calculated from TSex, C2, and the definition of Mach number.
- Stage exit static pressures (PSex) were calculated from stage exit total pressure, Mex, and isentropic relationships.

- Stage exit annulus areas (Aann) were calculated from mass flow (provided by BHGE's cycle summary, but not shown in Table 8), PHI, Up, TSex, PSex, and conservation of mass.
- The tip and hub diameters at the stage exits were calculated from Dp, and Aann.
- Vane exit flow angles (alpha1) were calculated from PHI, PSI, alpha2, and estimates of the ratio between vane exit and stage exit axial velocity (CZ1/CZ2) using velocity triangle relationships. Values of CZ1/CZ2 were derived from typical values seen in GE industrial power generation gas turbine (IGT) designs.
- Blade inlet relative flow angles (beta1) were calculated from alpha1, PHI, and CZ1/CZ2 using velocity triangle relationships.
- Blade exit relative flow angles (beta2) were calculated from PHI and alpha2 using velocity triangle relationships.
- Stage reactions were calculated from up, alpha1, alpha2, PHI, CZ1/CZ2, and C2. These were compared to the reactions reported by BHGE in Table 8. Deviations ranged between -3% and +2%, which is quite small considering that reaction levels are all in the 0.4 to ~0.5 range.

Table 8. Turbo-expander Stage Properties, Supplied by BHGE

Stage	1	2	3	4	5	6	7	8
P0 (bar)	11.607	10.164	8.818	7.402	6.208	5.008	3.96	3.105
H0 (kJ/kg)	875.4	852.4	828.3	799.4	771	737.5	701.9	666.4
T0 (Celcius)	519.1	501.8	483.5	461.4	439.6	413.6	385.8	357.7
V0	0.1682	0.1879	0.2115	0.2447	0.2832	0.3383	0.4105	0.5014
S0	6.8728	6.8762	6.8798	6.8842	6.8884	6.8934	6.8984	6.9034
X0	1	1	1	1	1	1	1	1
C0U (m/s)	0	-0.8	-7.6	-16.3	-11	-22.3	-23.9	-18.2
C0Z (m/s)	52	55.9	66.1	70.9	77	83.7	91.9	99.5
P1 (bar)	10.813	9.487	8.046	6.761	5.554	4.441	3.499	2.724
H1 (kJ/kg)	862.3	840	812.2	784	752.7	718.4	683.1	647.5
T1 (Celcius)	509.3	492.4	471.2	449.6	425.4	398.7	370.9	342.6
V1	0.1783	0.1989	0.2281	0.2636	0.3102	0.3732	0.4543	0.5579
S1	6.8737	6.8771	6.8809	6.8853	6.8898	6.8949	6.9001	6.9053
X1	1	1	1	1	1	1	1	1
C1U (m/s)	160.7	155.7	178.3	174.9	190.3	194.4	193.5	192.8
C1Z (m/s)	54.6	60.9	69.2	74.5	80.9	88.4	96.3	104.6
P2 (bar)	10.164	8.818	7.402	6.208	5.008	3.96	3.105	2.4
H2I (kJ/kg)	852.4	828.3	799.4	771	737.5	701.9	666.4	630.3
T2I (Celcius)	501.8	483.5	461.4	439.6	413.6	385.8	357.7	328.8
V2I	0.1879	0.2115	0.2447	0.2832	0.3383	0.4105	0.5014	0.6191
S2I	6.8762	6.8798	6.8842	6.8883	6.8933	6.8984	6.9034	6.9084
X2I	1	1	1	1	1	1	1	1
C2U (m/s)	-0.6	-7.4	-16	-10.7	-22	-23.6	-17.9	-13.1
C2Z (m/s)	55.8	66.1	70.7	76.9	83.5	91.7	99.4	108
H2S (kJ/kg)	849.7	825.7	796.2	768.1	734.1	698.6	663.3	627.4
ETAI	0.895	0.9	0.9	0.906	0.909	0.915	0.919	0.923
LAMBDA	2.1065	2.1256	2.4575	2.3004	2.5659	2.5655	2.4143	2.2775
PHI	0.3686	0.4323	0.4524	0.4814	0.5104	0.5462	0.5752	0.6066
PSI	2.2378	2.2929	2.6256	2.4552	2.7579	2.7527	2.5868	2.4632
M1	0.35	0.35	0.4	0.41	0.45	0.47	0.49	0.5
M2	0.33	0.36	0.39	0.4	0.45	0.47	0.49	0.51
U1 (m/s)	149.6	152.1	154.5	158	161.7	165.7	170.3	175.2
U2 (m/s)	151.4	152.8	156.4	159.8	163.7	167.9	172.8	178.1
Reaction degree	0.463	0.511	0.472	0.482	0.477	0.483	0.485	0.486

To complete the flow path cross section, airfoil axial chords are required. No guidance or indicators are provided from the BHGE data to size the airfoil chords, resulting in further design estimation. The following approximations, all guided by GE IGT historical ranges, were applied to size the airfoils:

- Airfoil loading coefficients (ZWI) of 0.8 and 0.9 were applied to all vanes and blades, respectively.
- All airfoil aspect ratios (AR, determined from airfoil height divided by airfoil axial chord) were held to between ~1.7 and 3.2. Vane ARs trended towards the lower end of this range, while blade ARs trended towards the higher end of this range (consistent with the small disparity in the applied ZWI values).
- All vane axial chord taper ratios (tip axial chord divided by hub axial chord) were set to 1.1, while all blade axial chord taper ratios were set to 0.9.

- Axial gaps between components were determine by ratios based on the axial chord of the upstream airfoil. Gaps between a vane and a downstream blade were set to 50% of the axial chord of the vane, and gaps between a blade and a downstream vane were set to 75% of the blade's axial chord.

Airfoil counts become an implied quantity from these assumptions. For the velocity triangles and geometry assumptions applied to the pilot expander, all vane counts fall between 30 and 40, while all blade counts fall between 40 and 60. These count ranges are well within bounds for typical small GE gas turbines. The flow path aerodynamic cross section derived from this calculation process is shown in Figure 19.

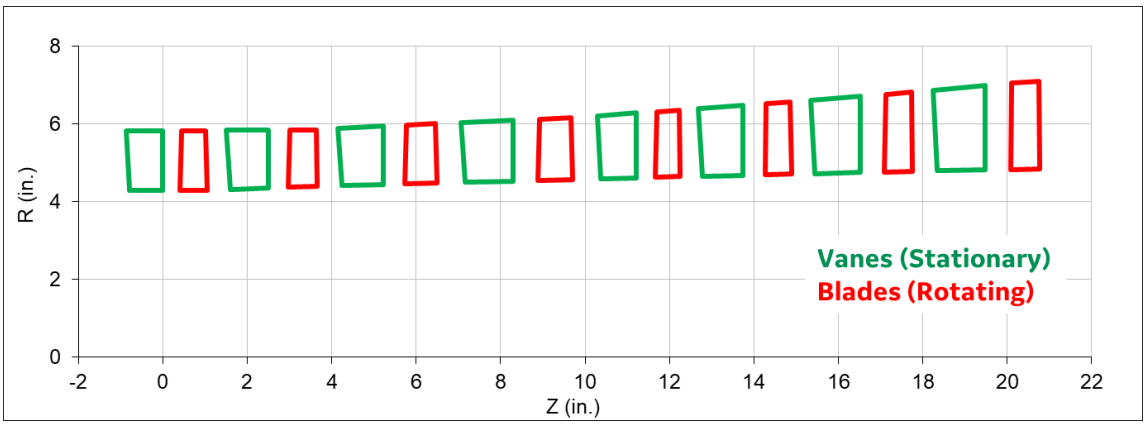

Figure 19. Approximated Turbo-expander Flow Path

With a flow path cross section, flow properties, and velocity triangles now available, detailed designs for the first stage and last stage airfoils were executed. Two separate through-flow models were generated using GE's proprietary streamline curvature code for turbine design: one for stage 1 that included vane 1 and blade 1, and one for stage 8 that included vane 8 and blade 8.

To execute the streamline design, the radial distribution of work must be defined. For simplicity and expediency, a free vortex work distribution (radius*tangential velocity = a constant along the airfoil span) was applied for both stages. Using the boundary conditions from the streamline curvature solution, airfoil shapes were defined at the hub, mid-span, and tip of the four airfoils of interest. As with the flow path design, reasonable assumptions based on GE IGT product experience were applied when designing the airfoil shapes. Figure 20 and Figure 21 show the airfoil designs for stage 1 and stage 8, respectively. Airfoil inlet property distributions related to the separator calculation are shown in Figure 22 and Figure 23 for stages 1 and 8, respectively.

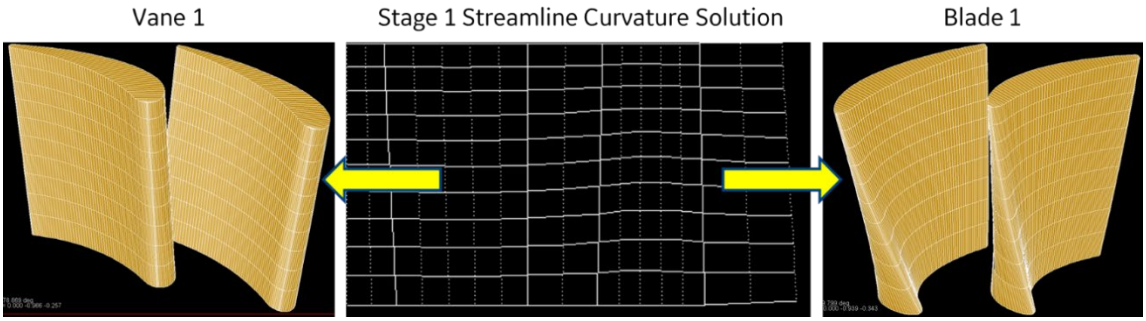

Figure 20. Stage 1 Streamline Curvature Solution and Airfoil Shapes

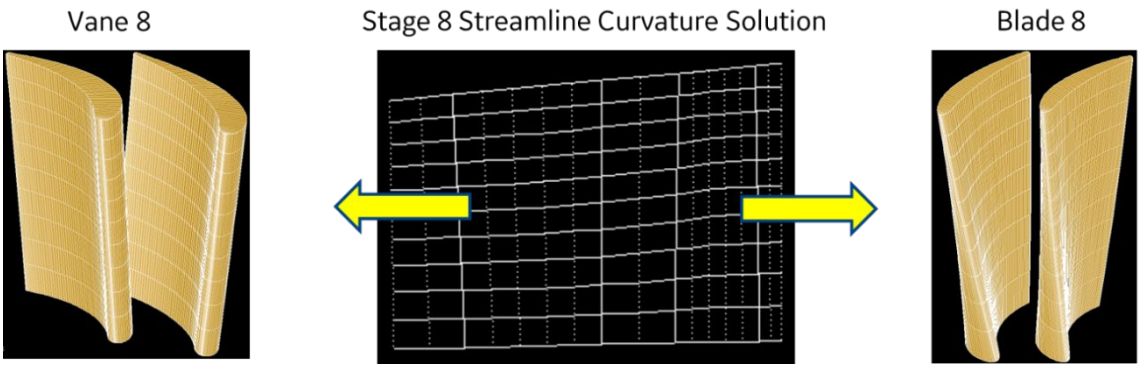

Figure 21. Stage 8 Streamline Curvature Solution and Airfoil Shapes

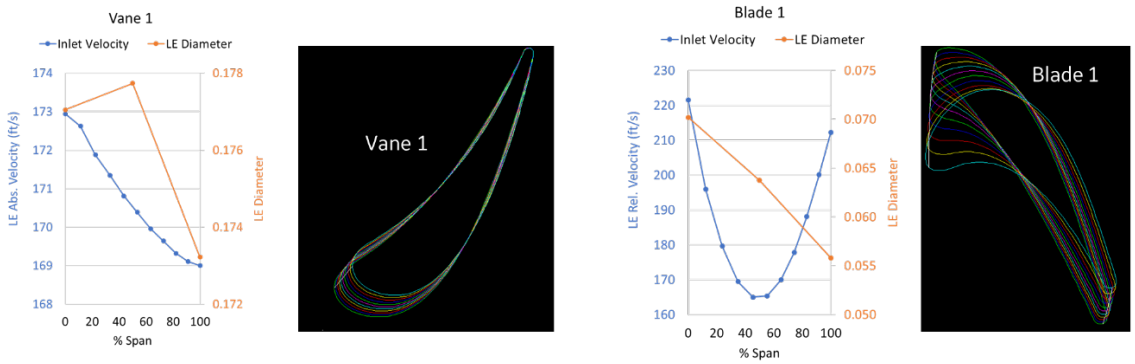

Figure 22. Stage 1 Airfoil Inlet Properties, Approximate Pilot Turbo-expander

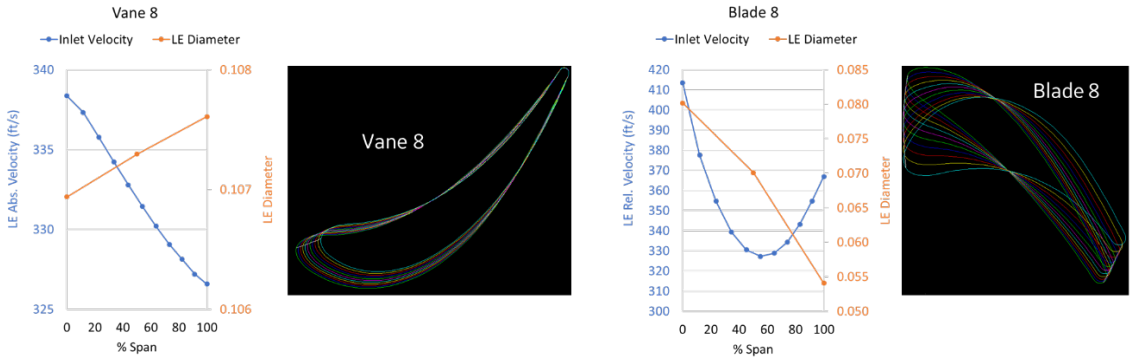

Figure 23. Stage 8 Airfoil Inlet Properties, Approximate Pilot Turbo-expander

3.2.4 COMMERCIAL SCALE ESTIMATE USING SCALED PILOT EXPANDER

The commercial scale plant has a substantially larger power output and mass flow than the pilot scale plant. While BHGE provided a turbo-expander design proposal for the pilot scale, no such proposal was obtained for a commercial scale turbo-expander. The velocity triangles and separator calculation inputs determined by the procedure detailed in section 1.1 will remain valid, as long as the turbo-expander is aerodynamically scaled from the pilot to the commercial size.

Typical IGT scaling rules were examined to best fit the pilot scale turbo-expander to the cycle requirements of the commercial plant. Generally, physical dimensions are scaled directly by a constant scale factor (SF). The turbine RPM scales by 1/SF, and mass flow, flow function, annulus

area, and power all scale by SF^2. To best bridge the gap between the pilot cycle and the commercial cycle requirements, a scale factor of ~6 was applied. Figure 24 shows the comparison between the pilot and commercial scale turbo-expander cycle requirements, along with the implied scale factor for each of the geometric or flow quantities of interest. Figure 25 shows an overlay of the pilot scale turbo-expander and an aerodynamically scaled turbo-expander that satisfies the commercial scale cycle requirements.

	Pilot	Commercial	Ratio	Implied SF
FF	4.25	137.83	32.41	5.69
Mass Flow	18.96	573.22	30.23	5.50
R_b1-tip	5.831	36.972	6.34	6.34
Exit A_ann	84.8	2988.2	35.26	5.94
Power (kW)	2154	90304	41.91	6.47
RPM	11000	2000	0.18	5.50
			avg aero SF	5.91

Figure 24. Cycle Requirements for Pilot Plant, Commercial Plant, and Implied Aerodynamic Scale Factor between These Two Cycles

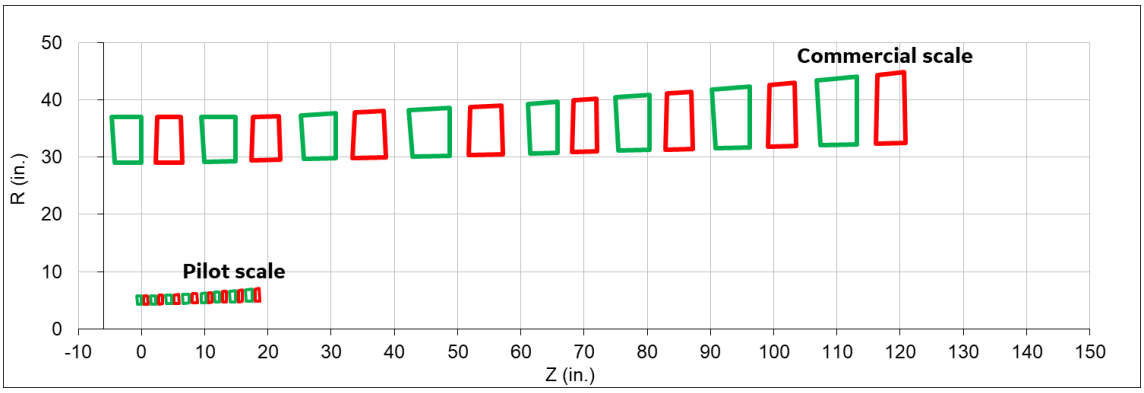

Figure 25. Overlay of Approximate Pilot Scale Expander and Aerodynamically Scaled Expander for Commercial Cycle Requirements

3.2.5 COMMERCIAL SCALE ESTIMATE USING ALTERNATIVE CUSTOM TURBINE DESIGNS

Apparent immediately in Figure 25 is the extreme length of the pilot plant turbo-expander design when aerodynamically scaled to the commercial flow and power requirements – over 10 feet of length from vane 1 leading edge to blade 8 trailing edge, before accounting for any additional length for the inlet duct or exhaust diffuser. Also, the RPM of the turbo-expander decreases from ~3 times grid frequency at pilot scale to 40% below grid frequency at commercial scale. Gearing or power electronics will, therefore, still be required to achieve the proper electrical frequency.

As an exploration exercise to define the limits of any potential separator requirements, several custom design turbo-expander flow paths rooted in GE IGT design practices were examined as well. The alternative flow path designs aim to decrease cost by: 1) decreased footprint and part count, and 2) grid-synchronized RPM to allow for direct drive of the generator, eliminating any requirements for gearing or additional power electronics. A high-speed (RPM > grid synchronous) flow path was also examined as an option to minimize the turbo-expander size (length and diameter) and to potentially examine the trade between turbo-expander cost and gear/electronics cost to convert the turbo-expander power to 60 Hz electrical frequency. The same design procedure described in section 1.1 was applied for the alternative flow paths; however, all stage parameters that were previously set by the BHGE data in Table 8 were purposefully varied.

The primary aerodynamic design changes applied to decrease the turbine footprint were the increase of shaft speed (from 2,000 rpm per the pilot scaling, to 3,600 rpm grid-synchronously), an increase of the stage loading coefficients, and an increase in the turbine average loading coefficient. Combined, these changes allow for more work (and pressure ratio) per stage, enabling a decrease in the total number of stages. Two flow paths were examined at grid-synchronous rpm (3,600) – one with four stages, and one with three stages. A three-stage flow path was also examined at 5,150 rpm to further decrease the turbo-expander size, primarily through reduction of the maximum diameter. All of the new flow paths adhere to the same cycle requirements as the scaled-up pilot plant turbo-expander.

Figure 26 shows an overlay of the approximate pilot, aerodynamically scaled commercial, grid-synchronous 4-stage, and grid-synchronous 3-stage turbo-expanders. The three and four-stage grid-synchronous turbo-expanders were designed to approximately the same average work coefficient (PSI), resulting in a lower average diameter for 4-stage flow path to produce the same total shaft power. The average work coefficients for the 3-stage and 4-stage flow paths shown in Figure 26 are approximately 0.7, which is only slightly higher than the pilot turbo-expander design (~0.6). Most of the work-per-stage increase comes from the increase in shaft speed. While both grid-synchronous flow paths have a modestly lower maximum diameter than the aerodynamically scaled pilot flow path, the overall length decreases dramatically – 60% shorter for the 4-stage flow path, 75% shorter for the 3-stage flow path. Besides length reduction, the grid-synchronous flow paths also reduce the total airfoil count by 40% to 45% due to the reduced stage count. The 3-stage flow path satisfies most typical IGT design limits, while the 4-stage flow path starts to exceed radius ratio limits for the last stage blade – a leading indicator that the last stage blade design would be very challenging, aerodynamically. The leading edge properties for separator sizing are included in Figure 27 and Figure 28 for stages 1 and 3 of the 3-stage grid-synchronous turbo-expander flow path.

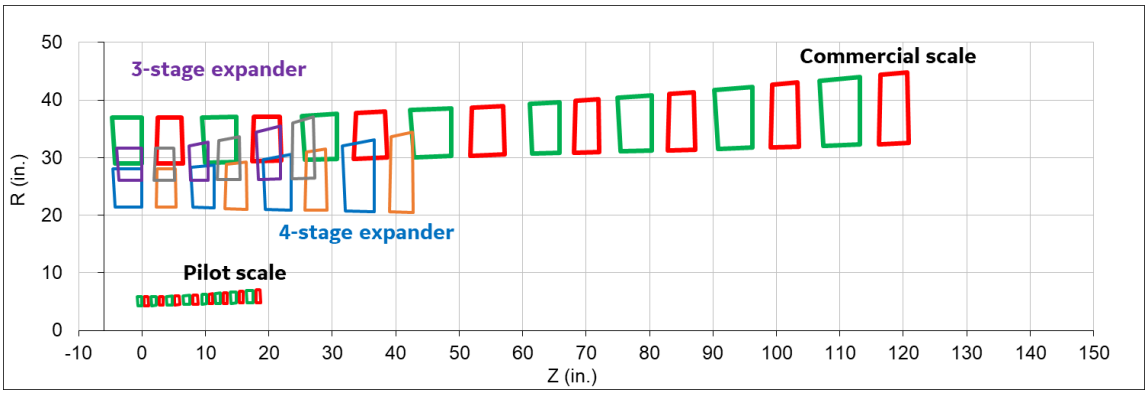

Figure 26. Overlay of Approximate Pilot, Aerodynamically Scaled Commercial, Grid-synchronous 4-Stage Commercial, and Grid-synchronous 3-Stage Commercial Turbo-expander Flow Paths

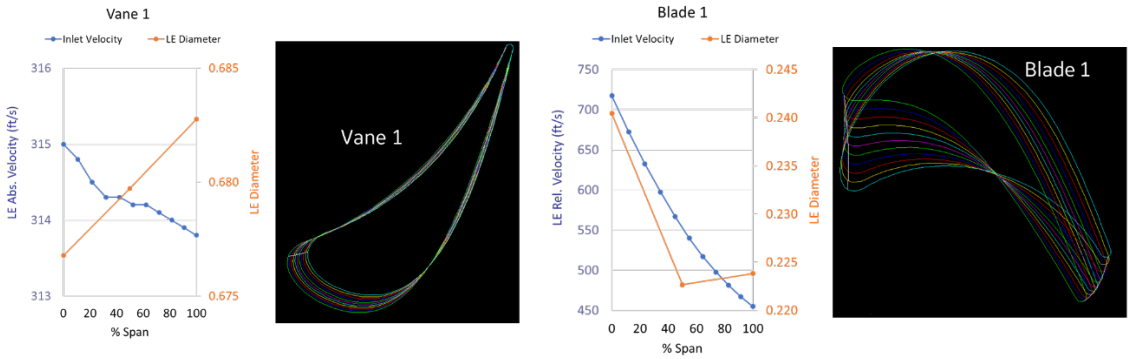

Figure 27. Stage 1 Airfoil Inlet Properties, 3-Stage Grid-synchronous Commercial Scale Turbo-expander

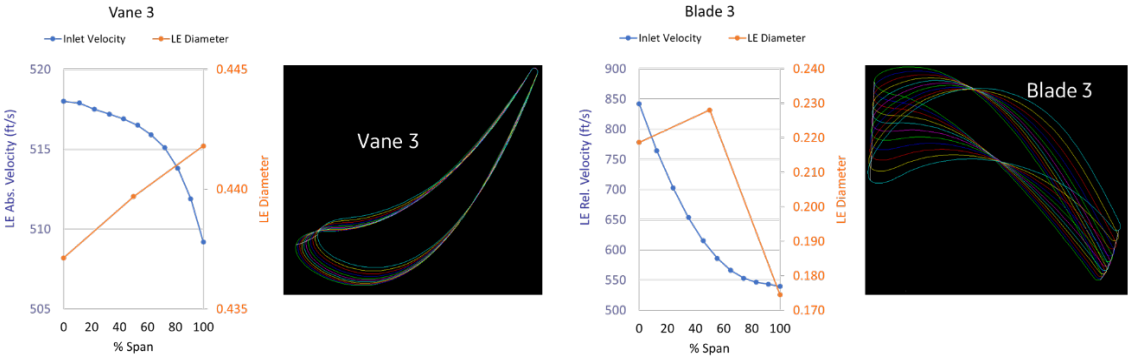

Figure 28. Stage 3 Airfoil Inlet Properties, 3-Stage Grid-synchronous Commercial Scale Turbo-expander

Figure 29 shows an overlay of the approximate pilot, aerodynamically scaled commercial, grid-synchronous 3-stage, and high-speed 3-stage turbo-expanders. The grid-synchronous and high-speed 3-stage flow paths are designed to the same average work coefficient, so the average flow path diameter ratio between these two designs trades directly with the inverse of the RPM ratio. Although the high-speed configuration minimizes the net turbo-expander flow path volume, the low inner diameter and high radius ratio of the last stage blade exceed typical turbine design limits, and efficient airfoil design will be highly challenged. Despite these practical challenges, the leading edge properties for separator sizing are included in Figure 30 and Figure 31 for stages 1 and 3 of the 3-stage high-speed turbo-expander flow path.

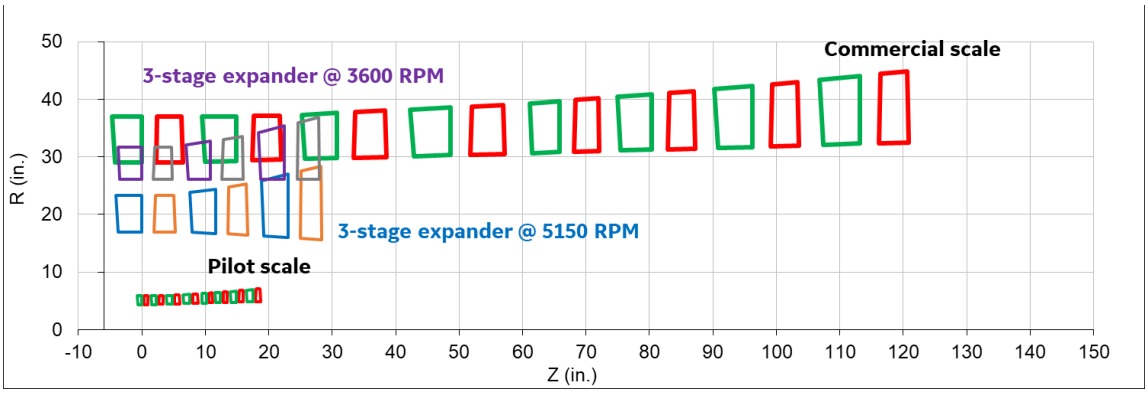

Figure 29. Overlay of Approximate Pilot, Aerodynamically Scaled Commercial, Grid-synchronous 3-Stage Commercial, and High-speed 3-Stage Commercial Turbo-expander Flow Paths

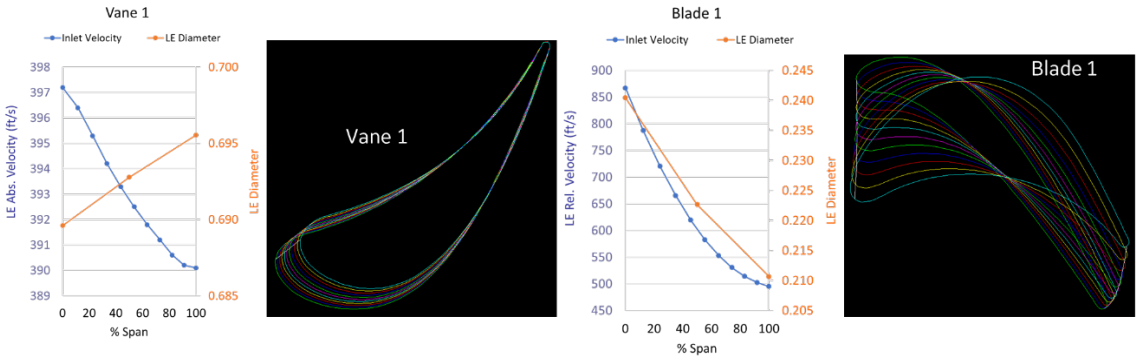

Figure 30. Stage 1 Airfoil Inlet Properties, 3-Stage High-speed Commercial Scale Turbo-expander

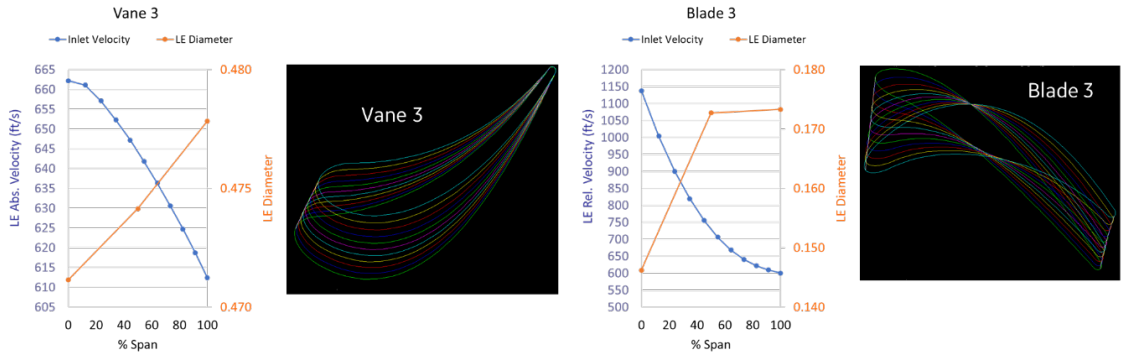

Figure 31. Stage 3 Airfoil Inlet Properties, 3-Stage High-speed Commercial Scale Turbo-expander

For the alternative, reduced-stage commercial flow paths, a full analysis of performance (efficiency) was not completed. Higher work coefficients as one could derive from a generic Smith chart typically result in lower efficiency. The higher Mach numbers associated with increased stage (and airfoil) pressure ratios also trend towards lower efficiency, including shocks at some local spans in the last stage of the 3-stage flow path. These effects would need to be more

rigorously assessed to perform a proper cost of electricity comparison between the different flow path designs.

In addition to efficiency, a more rigorous assessment of the detailed pressure field within each airfoil is required to ensure that undesirable effects, such as condensation, are not encountered. Since the airfoils of the reduced stage flow paths see higher pressure ratios and increased lift, the minimum pressures encountered within the airfoil passages are much lower in the reduced stage flow paths than the scaled pilot flow path. This effect can be seen by comparing the isentropic surface Mach number distributions, as shown in Figure 32.

Although many practical aspects of the reduced stage count commercial flow paths must be examined in more detail to verify feasibility, they provide in combination with the approximate pilot scale flow path a bounding range for the separator particle size cut-off calculation.

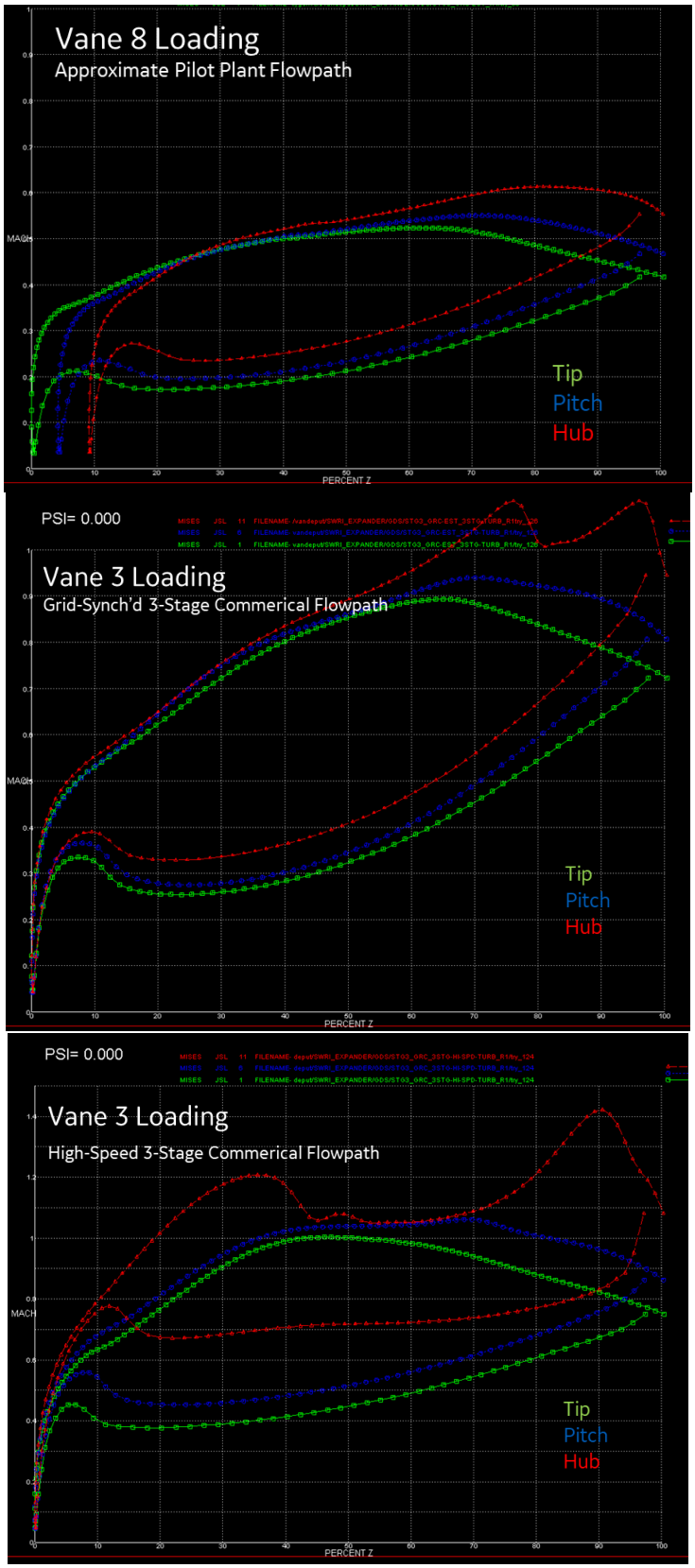

Figure 32. Isentropic Surface Mach Number Loading for Last Stage Vane

3.2.6 SEPARATOR PARTICLE SIZE CUT-OFF CALCULATION

Based on flow conditions and airfoil dimensions obtained from the turbo-expander aero design study, particle separation requirement is estimated using the methodology described in the approach section. This “cut-off” particle size calculations are performed for the first and last stage airfoils, both vane and blade, as a bounding condition. For each airfoil analysis, an averaged value over the airfoil span is used as a representative quantity.

Figure 33 shows the results of the “cut-off” particle sizes. In addition to 8-stage “baseline” turbo-expander architecture shown in blue, the results for two 3-stage turbo-expanders, 3,600 and 5,150 rpm designs, are presented as a design trade study in orange and gray, respectively. Although the 4-stage turbo-expander design is explored, it is considered as a less feasible design as explained in the prior section and excluded from this calculation.

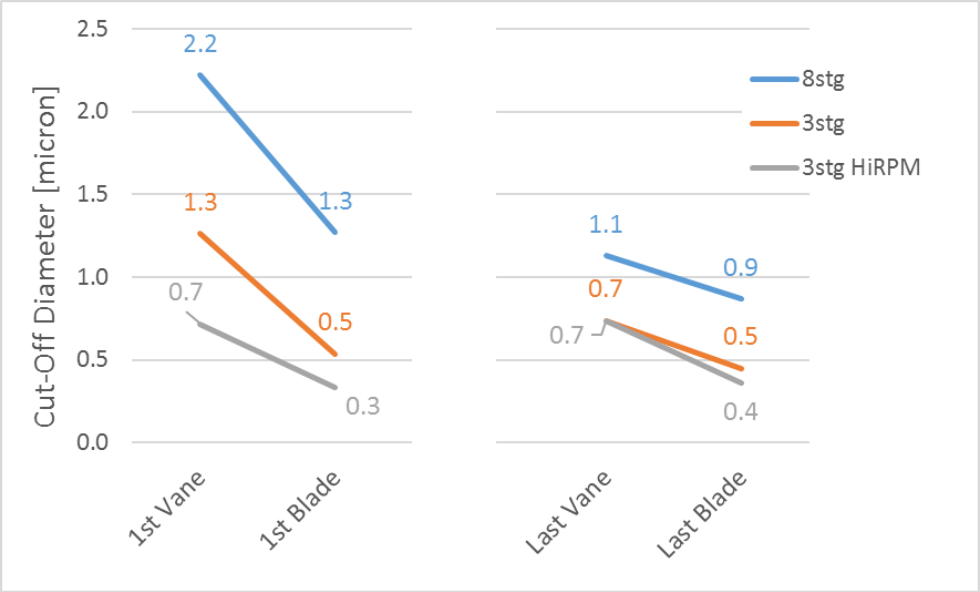

Figure 33. Calculated "Cut-off" Particle Size

Because the flow velocity within the turbo-expander changes by a much larger factor than the other parameters (dynamic viscosity and leading edge diameter) in Equation 1, the “cut-off” size is mainly driven by the flow velocity variation. Therefore, as the flow accelerates through the expander under all the designs studied, the minimum particle size having the erosion risk generally decreases from the first to the last stage. In other words, the last stage has a more “stringent” separation requirement than the first stage. For the 8-stage turbo-expander, the result shows that 2.2 microns and larger particles would collide with the stage 1 vane, and they need to be removed from the flue gas; in the same expander, 1 micron and larger particulates should be removed to reduce the erosion risk for the last (8^{th}) stage blade or the entire turbo-expander.

Among the turbo-expander designs investigated in the present study, “baseline” 8-stage turbo-expander will give the least “stringent” particle separation requirement that 1 micron and larger particles need to be removed. The 3-stage 3,600 and 5,150 rpm expanders will require a separator with a capability to separate down to 0.5 and 0.3 microns, respectively. Typically, removing finer particles is more challenging and costlier by an inertia-based separation device.

3.3 PARTICLE SEPARATOR SYSTEM EFFECTS

The commercial Aspen Plus system model was modified to include the separator. The changes to the system configuration are shown in Figure 34. The pressure drop is approximately 30 kPa, and the scavenge flow is 20% of the incoming flow. These parameters were informed by discussions with inertia particle separator vendors. The resulting system parasitic power requirements and losses are shown in Table 9.

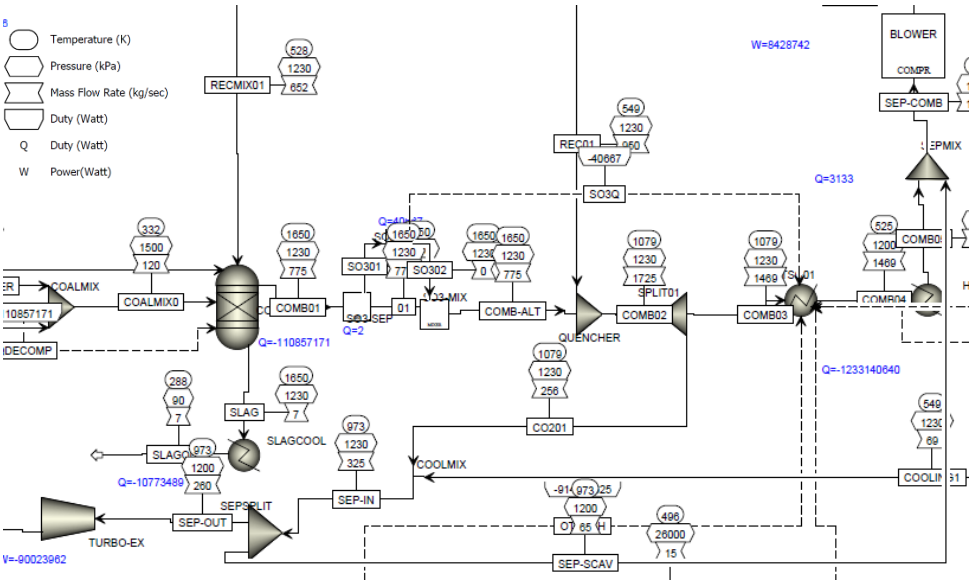

Figure 34. Modifications to the Commercial Aspen System Model Including the Separator

This change, for the same input, represents a loss of 0.08% efficiency in the system, which corresponds to a 1,459 kW electric loss. From the separator case, the team assessed the sensitivity of efficiency to scavenge flow. GE used this information to begin looking at the type of expander that would correspond with these commercial conditions. A reminder that the planned modularity is three combustion loops and three expanders to achieve the total heat input for this case. The expander input conditions are from the "SEP-OUT" stream: 800°C, 12 bar, 86.67 kg/s per expander (260.0 kg/s in total for all three expanders), and 20.34 m^3/s per expander (61.01 m^3/s in total for all three expanders). Composition of the streams was also produced by the Aspen Plus results.

Table 9. Power Balance for the FPO Commercial System with a Separator

Power Balance		
Heat Input		
Coal Feed Flowrate	299,390	kg/hr
Thermal input (HHV)	1,656,627	kWth
Thermal input (LHV)	1,596,083	kWth
Condenser Heat Duty	2,815	GJ/hr
Cooling water heat rejection	968	GJ/hr
Power Output		
Steam Turbine Power	664,191	kWe
Turbo Expander Power	90,024	kWe
Auxiliary Power Load		
HP Feedwater Pump	14,528	kWe
LP Feedwater Pump	182	kWe
Gas Recycle Blower	8,429	kWe
ASU Primary Fan	80,921	kWe
ASU Oxygen Compressor	32,651	kWe
ASU Auxiliaries	1,000	kWe
Air Condenser Fans (0.81% kWe/kWth)	6,334	kWe
Cooling Tower Fans (0.73% kWe/kWth)	1,962	kWe
Circulating Water Pumps (1.14% kWe/kWth)	3,064	kWe
Coal Bar Mill (18 kWe/kg/s coal)	1,497	kWe
Slurry Pump (7.7 kWe/kg/s coal)	640	kWe
Slag Handling (1.7 kWe/kg/s coal)	141	kWe
Steam Turbine Auxiliaries	329	kWe
Direct Contact Condenser Recycle Pump	34	kWe
Coal Handling and Conveying	629	kWe
FGD Auxiliaries (0.1% kWe/kWth)	16	kWe
Balance of Plant	2,000	kWe
Transformer Losses	2,629	kWe
CO2 Purification Loads		
CO2 LP Compressor Power	34,088	kWe
CO2 HP Compressor Power	14,390	kWe
Plant Performance		
Gross Power output	754,215	kWe
Net Auxiliary Load	156,987	kWe
Net CO2 Purification Load	48,478	kWe
Net Plant Power	548,749	kWe
Gross Power Efficiency (HHV)	45.5%	
Net Exported Power Efficiency (HHV)	33.1%	
Net Plant Heat Rate (HHV)	10,868	kJ/kWhr
Net Exported Power Efficiency without CO2 Capture (HHV)	36.1%	
Gross Power Efficiency (LHV)	47.3%	
Net Exported Power Efficiency (LHV)	34.4%	
Net Plant Heat Rate (LHV)	10,471	kJ/kWhr
Net Exported Power Efficiency without CO2 Capture (LHV)	37.4%	

3.4 SUITABILITY OF CYCLONES FOR PARTICLE COLLECTION

Cyclone separators have many advantages for the FPO turbo-expander application including low-pressure drop, high temperature, pressure capability, and low cost. In addition, they exhibit a smaller operational footprint and lower maintenance requirements than other technologies such as barrier filters. The team estimated the collection efficiency (Lapple model) for a 0.2 m diameter Stairmand high-efficiency cyclone geometry at a range of flow conditions expected at the 5-MWth pilot plant. Figure 35 shows a range of estimated 50% cut diameters of 7.4 µm to 3.3 µm for low- and high-flow conditions that may be considered representative of the performance achievable with traditional cyclone geometries. Based on the identified target of high-collection efficiencies for particles larger than 0.9 µm, non-concentrating high-efficiency cyclones cannot achieve adequate separation efficiencies for the FPO turbo-expander application.

Various recycle and concentrator schemes have been shown to increase particle collection efficiencies over traditional high-efficiency cyclones and are promising for the FPO turbo-expander application. These methods can generally be divided into two configurations: a collector-first with cyclone collector upstream of a concentrator, and a concentrator-first with cyclone collector downstream of a concentrator.

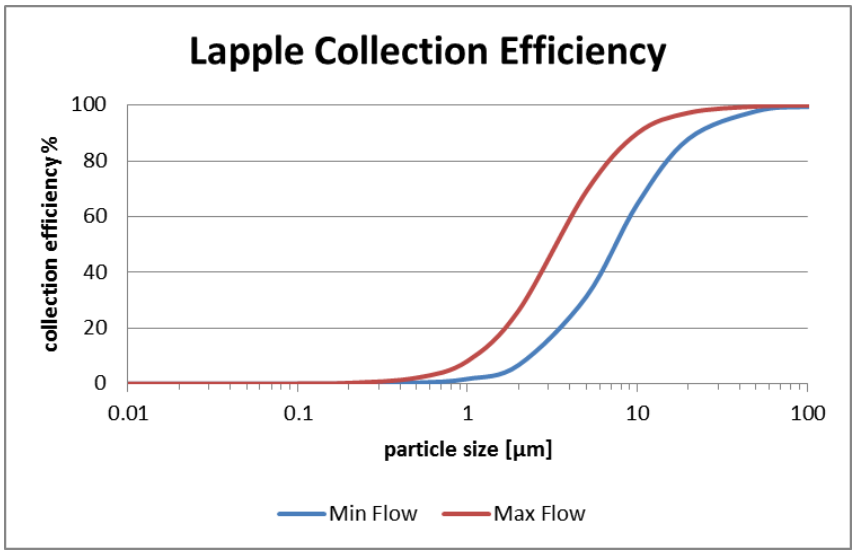

Figure 35. Lapple Collection Efficiency for 0.2 m Diameter Stairmand Cyclone at 5-MWth Pilot Flow Conditions

3.4.1 CONCENTRATOR-FIRST RECYCLE SCHEMES

Several recycle schemes with a concentrator followed by a reverse flow cyclone collector are described in the literature. European Patent No. EP0430647 and U.S. Patent US5180486 cover configurations of concentrator-first separators with various methods of recycle. U.S. Patent No.3257798 covers a similar concept developed for exhaust gas treatment of internal combustion engines. Figure 37 shows high collection efficiencies for particles in the micron range for the CORE™ Separator developed by Easom Corporation in Figure 36 with West-Virginia coal fly ash [7]. This system consists of a straight-through cyclone concentrator upstream of a reverse flow cyclone collector. It can have collection efficiencies higher than traditional recirculating cyclones when the concentrator efficiency (ηs) is greater than the collector efficiency (ηc). The overall efficiency can then be calculated by Equation 2 [8].

Equation 2.

$$\eta = \frac{\eta c \eta s}{1 - \eta s + \eta c \eta s}$$

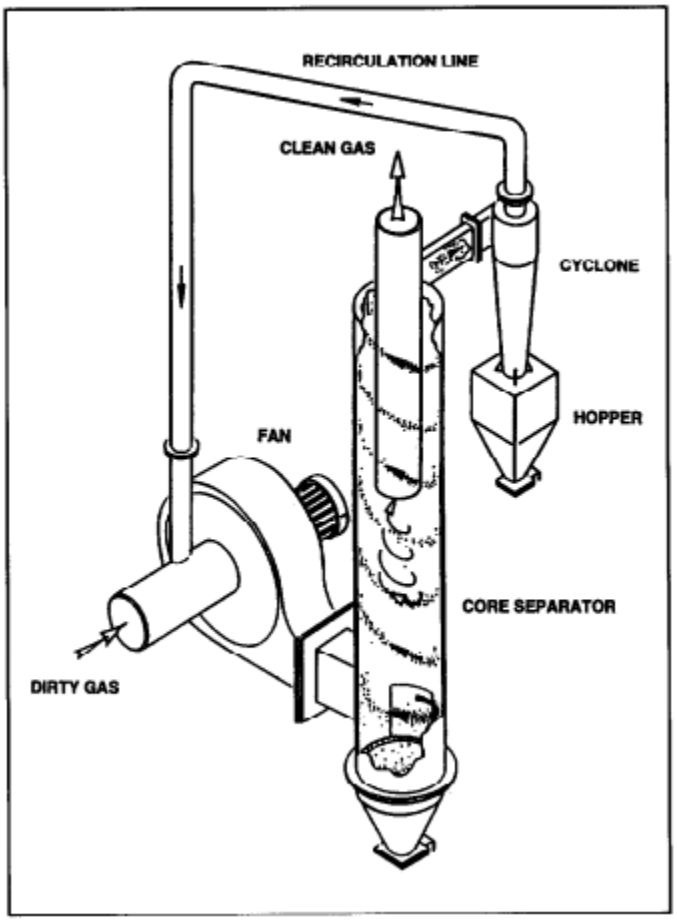

Figure 36. CORE Separator™ Concentrator-First Recycle Scheme [7]

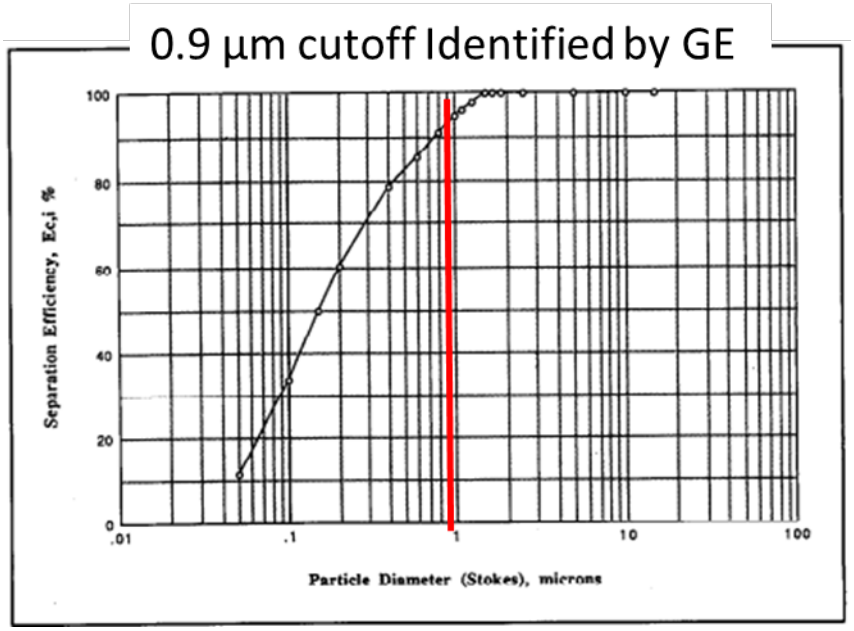

Figure 37. CORE Separator Efficiency – West Virginia Coal Fly Ash [7]

3.4.2 COLLECTOR-FIRST RECYCLE SCHEMES

When the cyclone collector is placed upstream of the concentrator within a recycle loop, the system will always have a collection efficiency greater than a single reverse flow cyclone or a concentrator-first loop as calculated by Equation 2.

Zhao et al. [9] showed significant improvements in collection efficiencies for sub-micron particles for a Post-Cyclone (PoC) concentrator with a recycled bleed flow fitted to the outlet of a reverse flow cyclone collector [9]. The PoC consists of two cylindrical shells in an annular configuration fitted to the vortex finder-outlet of a reverse-flow cyclone as shown in Figure 38. It makes use of the swirling flow from the vortex finder-outlet to provide further separation, and efficiencies can be increased with the inclusion of a recycle loop. Figure 39 shows high collection efficiencies of the PoC with 20% bleed flow for particles in the micron range.

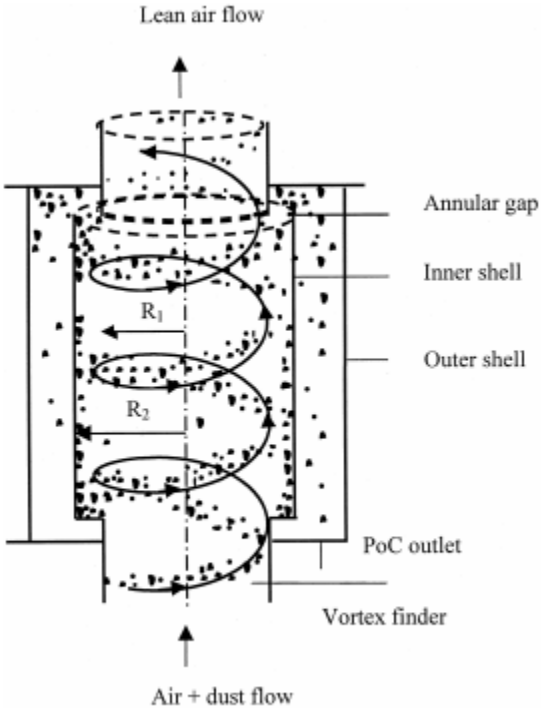

Fig. 1. A schematic illustration of dust flow in the PoC.

Figure 38. PoC Schematic [10]

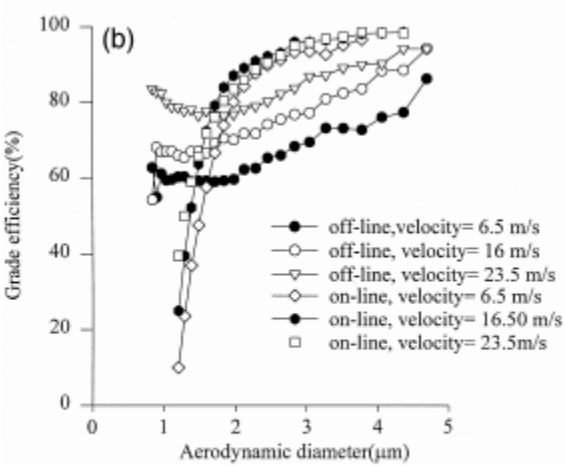

Fig. 4. (a) Overall collection efficiency of the cyclone and PoC at different inlet velocity. (Bleed flow = 20%) (b) Grade efficiency of the test cyclone at different inlet velocity shown by two methods.

Figure 39. Overall Collection Efficiency of a Cyclone and PoC [9]

The closed recovery system (CRS), as shown in Figure 40, uses a centrifugal concentrator downstream of a reverse flow cyclone collector to increase collection efficiencies within a recycle [11]. Collection efficiencies for below 5-micron particles have not been evaluated. Further development would be needed to assess the suitability of this technology for the FPO separator.

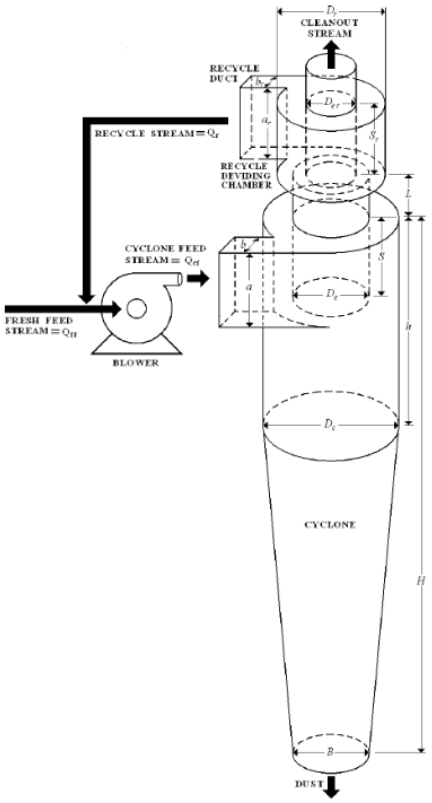

Figure 1. The schematic illustration of the CRS scheme.

Figure 40. CRS Centrifugal Device Downstream of Recirculating Cyclone [11]

The ACS system uses a straight-through cyclone downstream of a numerically optimized recirculating cyclone to increase collection efficiencies of sub-micron particles via a collector-first recycle. Electrostatic elements can also be included to increase the separation efficiencies for small particles. The ACS system has been demonstrated at the pilot and industrial scales and is the best available technology for cyclone separation of sub-micron particles [8].

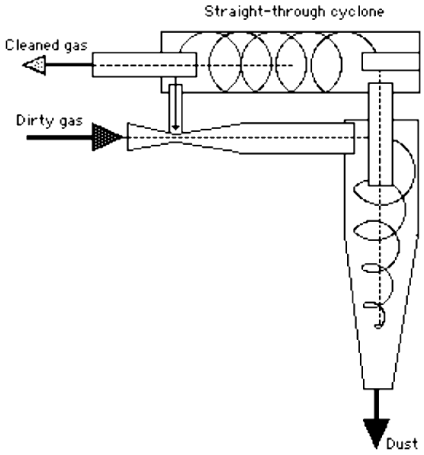

Figure 3. Proposed collector-first recirculation system.

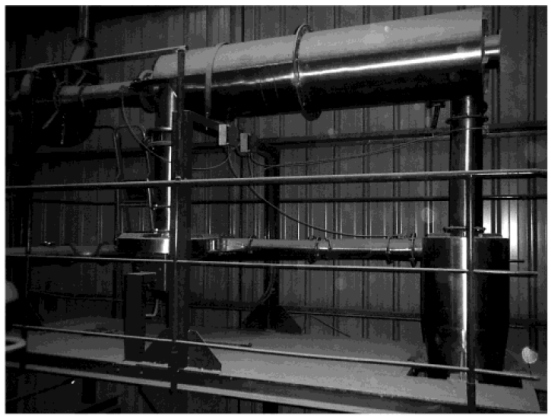

Figure 4. Pilot-scale system (RS_VHE cyclone and concentrator).

Figure 41. ACS Cyclone System Concept and Pilot-scale Configuration [8]

3.4.3 MODELING METHODS FOR NUMERICAL OPTIMIZATION OF CYCLONE SEPARATORS

Salcedo et al. [8] have demonstrated the use of recirculating numerically optimized cyclone designs for fine particle capture in biomass boilers [12]. By numerically optimizing the collector-concentrator system, significant increases in collection efficiencies can be achieved for micron scale and sub-micron scale particles. Numerical optimization is achieved within primary constraints on geometry, collection efficiency, pressure drop, and saltation velocity.

Ramachandran et al. [13] give an empirical model for pressure drop within a reverse flow cyclone separator, which is adopted by Salcedo et al. [8] as an optimization constraint. As shown in Equation 3, the saltation velocity constraint is used to limit particle re-entrainment [14].

Equation 3.

$$\frac{u_{in}}{u_s} < 1.25$$

$$u_s = 4.912\left(\frac{4g\mu\rho_p}{3\rho}\right)^{\frac{1}{3}}\left[\frac{\left(\frac{b}{D}\right)^{0.4}}{\left(1-\left(\frac{b}{D}\right)^{\frac{1}{3}}\right)}\right]D^{0.067}u_{in}^{\frac{2}{3}}.$$

Mothes and Löffler [15] predict collection efficiency for reverse flow cyclone separators depending on an empirical parameter; the particle turbulent dispersion coefficient [15]. Salcedo et al. [12] adopted the model to calculate the collection efficiency for a recirculating collector-concentrator system as shown in Figure 42. The Salcedo method is an iterative solution, where the particle size distribution through the collector and the concentrator is changed in each iteration. The turbulent dispersion coefficient (D_r) in the Mothes and Löffler model is adapted to unknown

geometries through an empirical correlation between the radial Peclet and Reynolds numbers as given in Equation 4 [14].

Equation 4.

$$\mathrm{Pe_p} = 0.0342\ Re_p^{1.263}$$

$$Re_p = \rho d_p w / \mu$$

$$\mathrm{Pe_p} = w d_p / \mathcal{D}_r$$

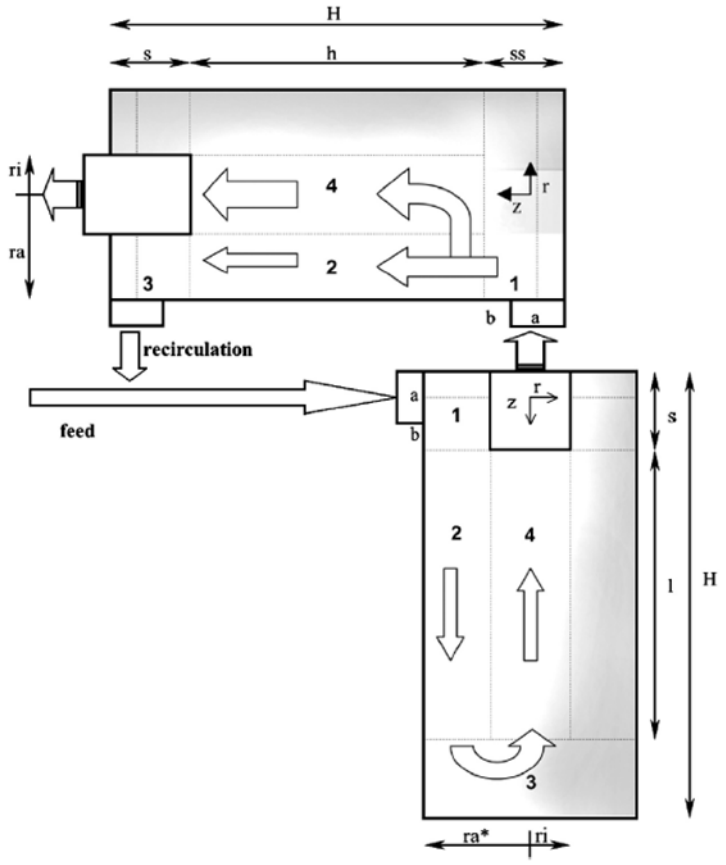

Fig. 1. Geometric model for proposed recirculation system.

Figure 42. Geometric Model for Salcedo et al. Numerical Optimization [12]

3.5 DESIGN DEVELOPMENT OF THE CYCLONE SEPARATOR

Based on a review of the literature and best-available commercial technology, traditional high-efficiency reverse flow cyclone separators are not well suited for the FPO turbo-expander application due to poor collection efficiencies at small particle sizes. Significant improvements can be made for micron-scale particle collection by combining a reverse flow cyclone separator with an upstream or downstream concentrator via a recycle loop. By numerically optimizing the

cyclone collector, further improvements can be made to yield an ideal combination of low-pressure drop, high collection efficiency, and low construction, maintenance, and operating cost.

Promising technologies after the evaluation process were the Advanced Cyclone Systems (ACS) and the CORE Separator System. The team worked with potential vendors to investigate potential off-the-shelf or semi-custom solutions for the separator. Methods developed and experimentally validated by Salcedo et al. [12] were applied to study the system.

3.5.1 DESIGN CONDITIONS FOR THE 5-MWTH PILOT DEMONSTRATION

The particle separator vendor developed a proposal for the 5-MWth pilot based on the following design conditions.

- Pressure: 3.10 to 4.48 barg
- Temperature: 500°C to 650°C
- Flue gas flow rate:
    - Min: 141.6 N l/s
    - Avg: 339.8 N l/s
    - Max: 424.8 N l/s
- Separation requirements: High separation efficiency for particles ~1 µm and larger

3.5.2 ADVANCED CYCLONE SYSTEMS (ACS)

The team engaged ACS systems to develop a proposal for a collector-first recycle scheme based on the ACS Hurricane Cyclone System.

The performance of the ACS ReCyclone is shown in Figure 43 with the new area of interest for particle removal highlighted. A cyclone with concentrating characteristics, such as the ACS ReCyclone, may achieve removals of 80%.

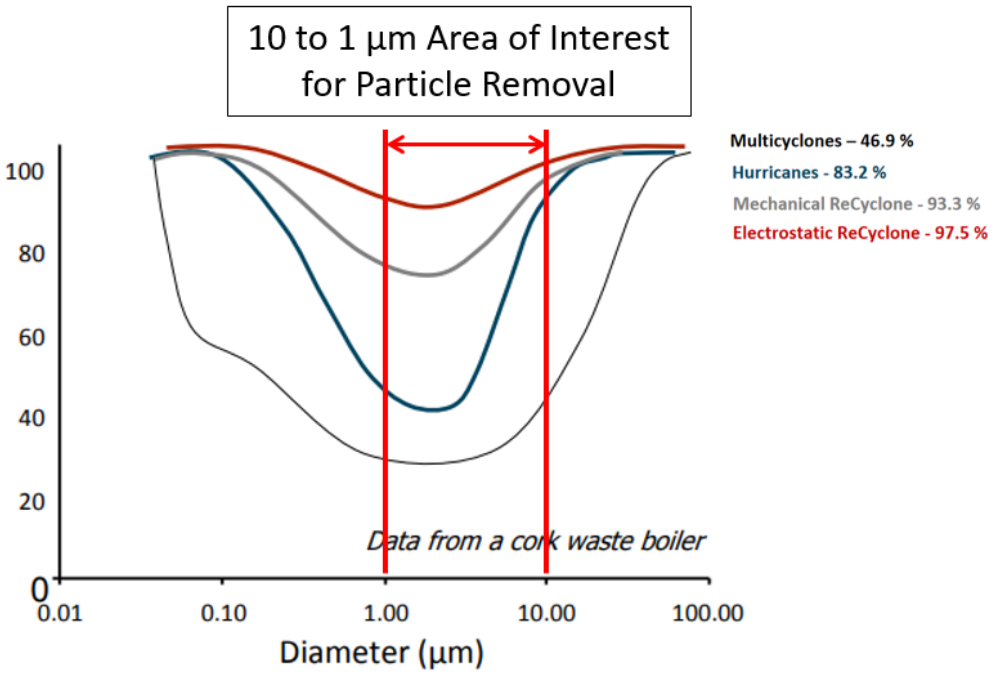

Figure 43. Updated Region of Interest for FPO Particle Removal

The concept proposed to achieve high separation efficiency for a cyclone is shown in Figure 44. The incoming flow is directed into a “hurricane” cyclone, where the flow exits the top. This flow is passed through a secondary concentrator cyclone. This cyclone returns some of the particles to the “hurricane” cyclone. This should provide the removal efficiency required to extend the life of the turbo-expander.

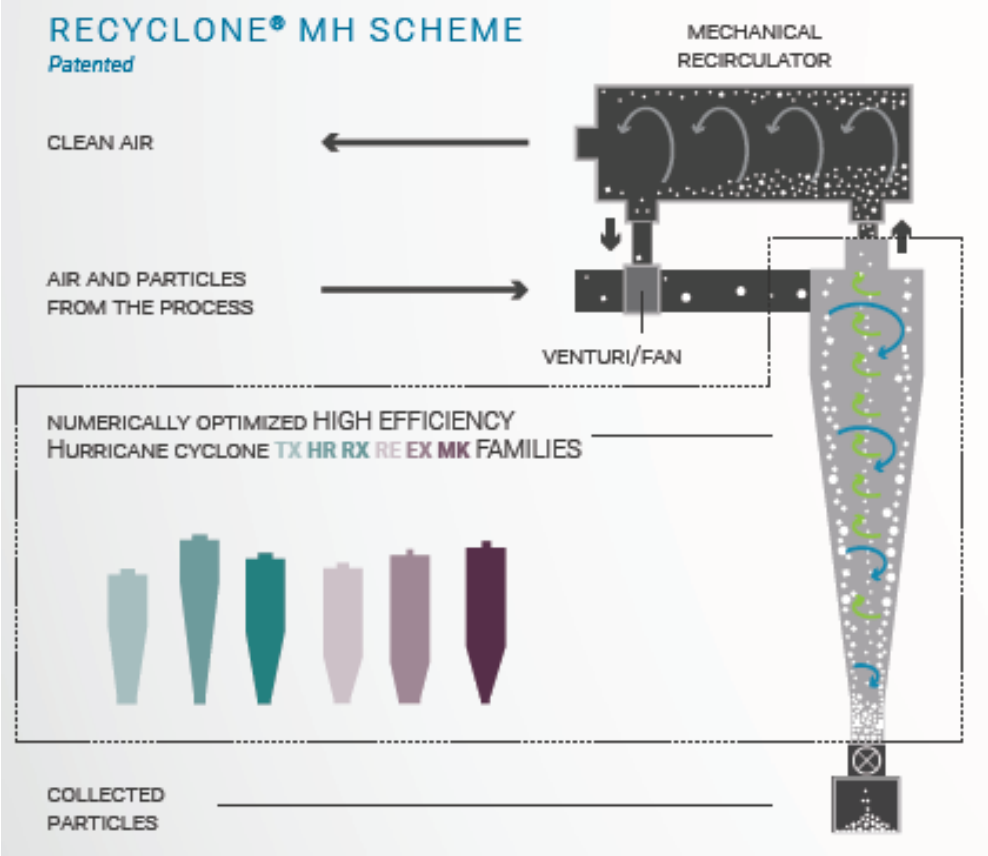

Figure 44. Proposed Advanced Cyclone Design

The team developed a data sheet for the specification of the ACS cyclone system and submitted it to the vendor.

3.5.3 POSSIBLE MODIFICATIONS TO THE ACS RECYCLONE TO IMPROVE PERFORMANCE

There are several proposed modifications that could improve the cyclone separation efficiency. In order to accommodate higher cycle efficiency, the system should allow up to 650°C. This could be achieved with alloys that maintain higher strength at these temperatures. Cooling of metal walls to protect metal could also improve the strength of more standard construction materials. An additional benefit of cooling is that it could create cool fluid near wall. Cool flue gas near wall creates a gradient of viscosity which lowers the viscosity. Lower viscosity near the wall could increase the Stokes number and improve separation efficiency. These proposed changes were designed and implemented based on feasibility and predictions of numerical analysis.

3.5.3.1 About Hurricane® Cyclones

Hurricane cyclones are patented numerically optimized cyclones. Hurricane geometries maximize powder collection for each application, while minimizing re-entrainment and keeping pressure drop at reasonable levels. Hurricane cyclones demonstrate impressive efficiencies in capturing very fine powders with a Median Volume Diameter (MVD) of less than 5 µm. These cyclones are the output of nonconvex nonlinear problems formulated and solved after years of work in partnership with the Faculty of Engineering of Porto (FEUP). A single Hurricane is more efficient than any other known cyclone available in the market for the same pressure drop.

In 2013, a better understanding of agglomeration in cyclones has allowed ACS to offset all its products to another level. ACS has launched a completely new line of cyclone geometries, different from any other in the world - named Hurricane MK, which has already proven to represent a giant leap in terms of efficiency. Please see more information on the ACS website for reference lists regarding installations of ACS systems worldwide for applications that go from pharmaceuticals, chemicals, and food ingredients to mineral industries.

Figure 45 Pictures of Different ACS Cyclones

3.5.3.2 Project-Related Specification and Operating Conditions / Design Data

- Type of powder [vitrified slag + ash]
- Particle apparent density dS (g/ml) [2.7]
- Particle size [provided by the client]

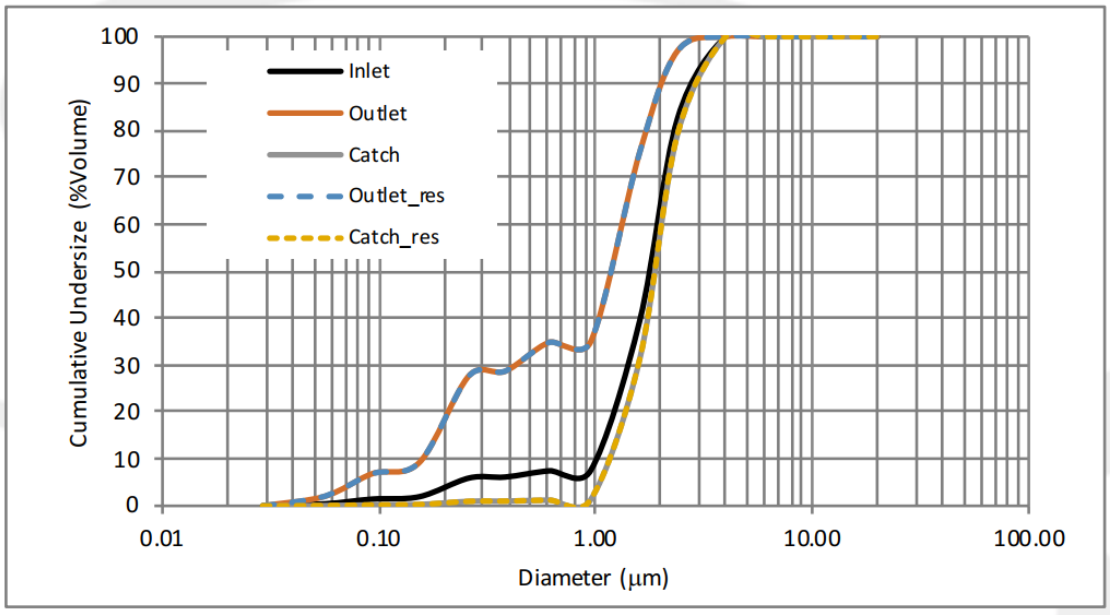

Figure 46. Particle Size Distribution of FPO

- Design flowrate (m^3/h | Nm^3_{dry}/h) [648 | 1 021]
- Solids content (mg/m^3 | mg/Nm^3_{dry}) [95 | 60]
- Gas temperature (ºC) [503]

3.5.3.3 Performance Results

- Expected captured efficiency (%) [73.1 – 89.8]*
- Expected pressure drop only in the cyclones (kPa) [10.4]
- Expected emissions (mg/m^3 |mg/Nm^3_{dry}) [10 - 26 | 6 - 16]
- Guaranteed emissions (mg/Nm^3_{dry}) [≤20]

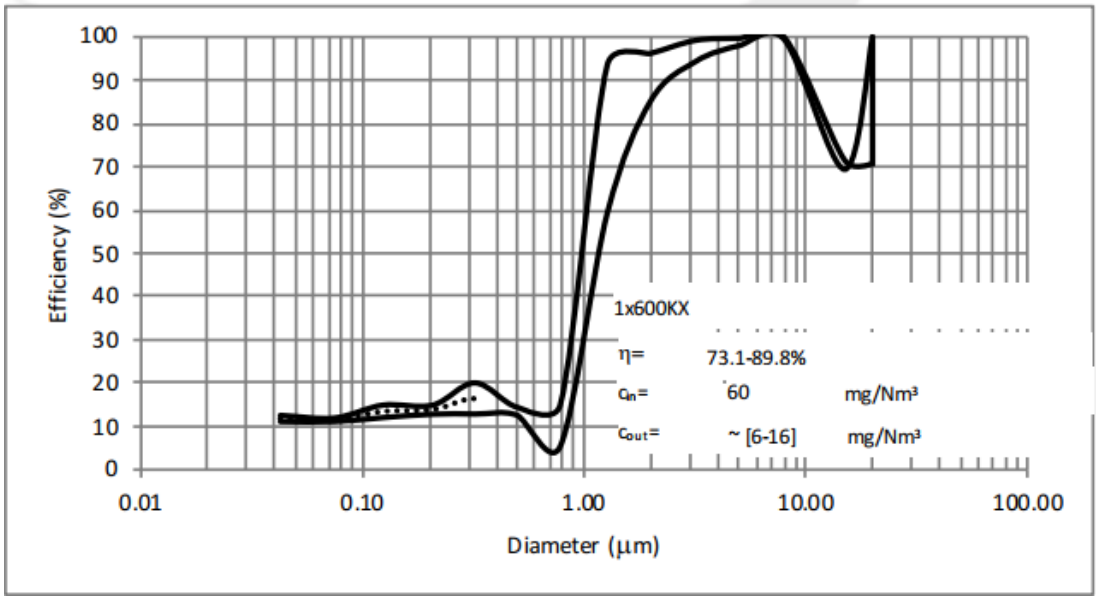

Figure 47. Predicted Grade and Global Efficiency for 1KX600

3.5.3.4 Hurricane Specifications and Dimensions

- Diameter (mm) [600]
- Material [AISI 304L]
- Thermal insulation [No]
- Internal and external surface finishing (µm): [2B]
- Internal welds (µm): [Ground smooth to Ra < 0.8, welded TIG and passivated]
- External welds (µm): [Ground, welded TIG and passivated]
- Radius of polished weld at internal angles (mm): [3]
- All gas inlet, gas outlet and solids outlet are flanged
- Gaskets in Sigraflex HD or equivalent
- Discharge pipe
- CE marking on the cyclone
- PED2014/68/EU category III – Mod G (pressure vessel)
- Calculations done both for the PED and American Society of Mechanical Engineers (ASME) Sec. VIII Div.1
- ACS drawings were provided to Client for review/approval before the manufacture of the cyclone. Only after Client approval of the drawings would fabrication proceed. Material certificates documentation, instruction, and operation manual in English.

More specific manufacturing details were defined with the project team during the detailed drawing phase.

3.5.3.5 Overall Dimensions

Preliminary approximate dimensions* are:

Table 10. General Dimensions of the Cyclone

System configuration	W Width (mm)	H Height (mm)
KXø600	600	1600

(*) All dimensions pendent of confirmation by detailed drawings for approval which were submitted by ACS after placement of the order.

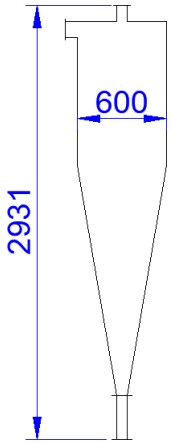

Figure 48. General Dimensions of the Cyclone

3.5.4 ACS Purchase Order and Beginning of the Detailed Design

Costs were checked and compared against competing companies. However, as discussed previously in Section 3, the ACS cyclone was the only technology that was found to provide the desired performance of particle separation while operating at the loop conditions and not introducing the risk of clogging, as is found for FPO with ceramic barrier separators. Furthermore, the ACS equipment was quoted at a cost lower than the ceramic candle filter.

3.6 DESIGN FOR FABRICATION OF THE PARTICLE SEPARATOR

The team worked with ACS cyclone, the commercial vendor for development, fabrication, and delivery of the particle separator. The team worked to ensure that the design followed the specifications from the original ACS proposal. The design underwent reviews to ensure the design is de-risked for the application, including pressure temperature and volumetric gas flow. The particle separation efficiency of the design can be verified in a test campaign.

Here is a broad description of the design features: The separator inner diameter (ID) is 600 mm with a typical wall thickness of 5 mm. The height of the separator from top outlet pipe to bottom discharge pipe exit is 3,114 mm. The head of the separator is a Klopper Dished head with a 600 mm ID. The outer diameter (OD) of the top outlet pipe and the bottom discharge pipe are 76.1 mm, and the OD of the inlet pipe is 114.3 mm.

ASME Section VIII Division 1 is used as the governing code for pressure vessel design. The design pressure is 6 bar(g), and the vessel was subjected to a hydraulic pressure test up to 20 bar(g). The maximum design temperature is 565°C.

The empty weight of the design is 250 kg with a 740 kg water weight. This corresponds to a separator volume of 490 L. The equipment is supported by c-channel brackets on the sides of the vessel and a mounting plate on the front of the separator near the inlet port.

Generally, the body is typically made from American Society for Testing and Materials (ASTM) A240 grade 304L stainless steel. Piping is typically made from ASTM A312 TP 304L stainless steel.

The design was matured with more detail including lifting points and positioning of the structural mounts. The design also includes flange locations for inlet, gas outlet, and particle outlet.

3.7 COMPLETION OF PARTICLE SEPARATOR FABRICATION

ACS completed the fabrication of the particle separator. Some of the images of the fabricated separator are shown in Figure 49 through Figure 52.

Figure 49. View of Particle Separator Body in Box for Shipping

Figure 50. View of Support Bracket for Particle Separator Mounting

Figure 51. View of Outlet Flange and Trap for Particle Collection

Figure 52. View of Particle Separator Nameplate and Inlet Flange

4. INTEGRATION INTO THE EXISTING TEST FACILITY

The project team made progress in preparing the host site to accommodate the test. The engineering, purchasing of equipment, and modification of the test facility are detailed in this section.

4.1 DEVELOPING THE FACILITY MODIFICATIONS

The 5-MWth plant in Italy is the planned location for the demonstration test. ITEA had begun to scope the modification required.

4.1.1 BLOCK FLOW DIAGRAM FOR THE CYCLONE TEST

A preliminary integration into the test facility is provided in Figure 53. The hot flow prior to the boiler inlet is diverted and mixed with flow from the recycle blower outlet. This passes through the cyclone, and particulate matter is removed. After the cyclone, the flow is split between a cooler and a smaller flow that passes through an ELPI. The flow is recombined and supplied to the flue gas treatment equipment before it is sent to the stack.

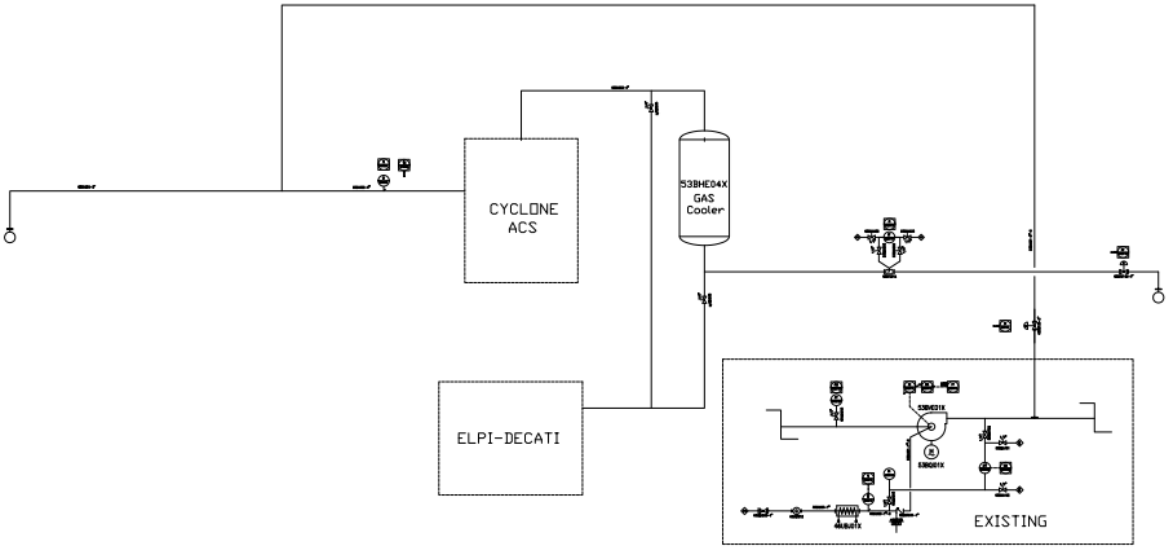

Figure 53. Block Flow Diagram of the Proposed Facility Modification

4.1.2 FACILITATION OF COMMUNICATION BETWEEN SUPPLIER AND HOST

Project management developed a non-disclosure agreement between ITEA and ACS. This allowed the groups to communicate more deeply on the cyclone design and facilitate the installation at the test facility. This arrangement would also allow ACS access to data from ITEA and allow for future improvement on the performance of the technology.

4.1.3 PROPOSED MODIFICATIONS TO THE 5-MWTH PILOT

The project team worked on developing the modifications needed for integration at the host site. The preliminary proposed modifications are shown in Figure 54 through Figure 56

A description of the modifications is provided below:

- Line 53BA050 -3″ – Stainless Pipe 3″ – Sch STD – ASTM A 312 Tp 304
    - This pipe starts from 16″ hot flue gas stainless (from combustor-quencher) pipe closed to the inlet nozzle (tubes side) of 1st heat-exchanger Boiler.
- Line 53BA051 -3″ – Stainless Pipe 3″ – Sch STD – ASTM A 312 Tp 304
    - This pipe starts from 10″ Quencher Recycle carbon steel pipe.
- Node 1 – This is the point where line 53BA050 -3″ and line 53BA051 -3″ meet. From this point stars a new 4″ line.
- Line 53BA052 -4″ – Stainless Pipe 4″ – Sch STD – ASTM A 312 Tp 304
    - This pipe starts from Node 1 with quenched flue gas. It arrives up to the 53BHE04X ACS Cyclone
- ACS CYCLONE
    - To install this element the team would increase the steelwork adding a new “balcony” with the support.
- Line 53BA053 -4″ – Stainless Pipe 4″ – Sch STD – ASTM A 312 Tp 304
    - This pipe starts from Cyclone. It arrives up to the 53BHE04X Gas Cooler Heat Exchanger
- 53BHE04X Gas Cooler Heat Exchanger
    - A TEMA BEM type vertical heat exchanger. It would be placed in an existing free corner
- Line 53BA054-4″ – Carbon steel Pipe 4″ – Sch STD – ASTM A 106 gr. B – this pipe starts from 53BHE04X Gas Cooler Heat Exchanger and arrives at the lamination valve 53BRE04X (close to the blower) that would reduce the pressure to head needed for FGD tower and stack pressure drop
    - After the lamination valve, the flue gas would proceed to de-acidification tower and stack.
- The ELPI-DECATI is the instrument that investigates about the quantity of dust. It needs a ¼″ lines that would be installed before the test.

The length of stainless steel lines is due to the thermal elongations and preliminary calculations. The actual length would be decided after final stress analysis.

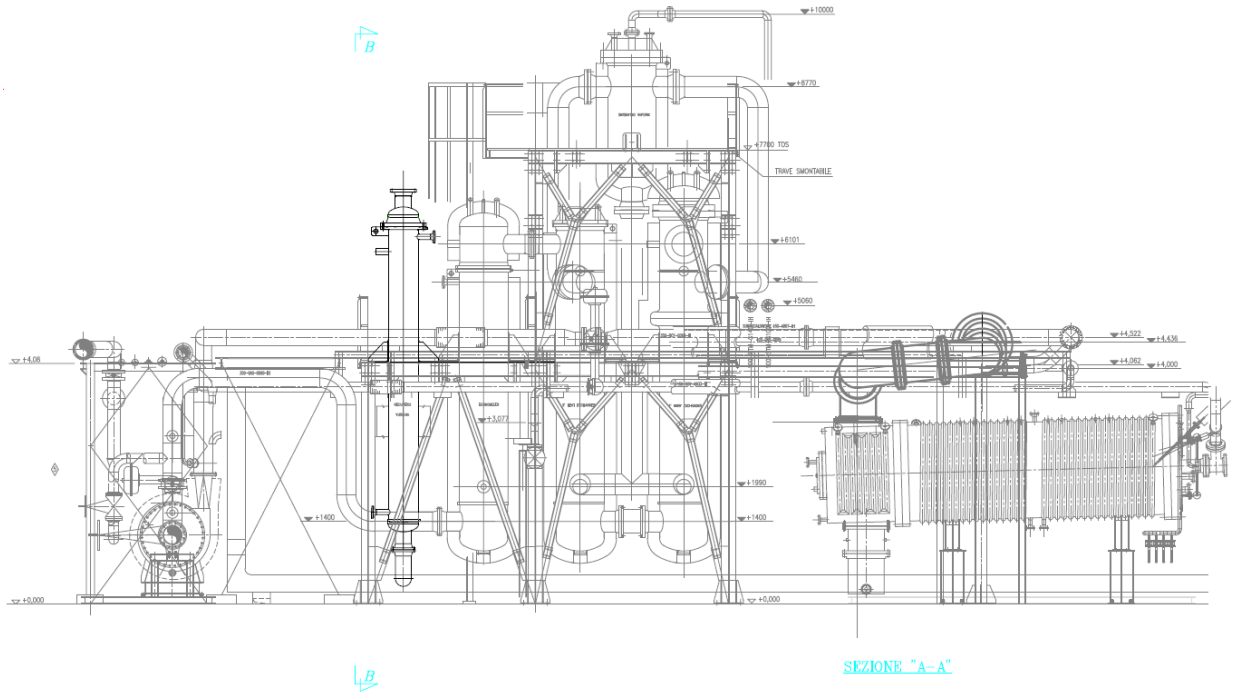

Figure 54. Proposed Facility Modification: Front View

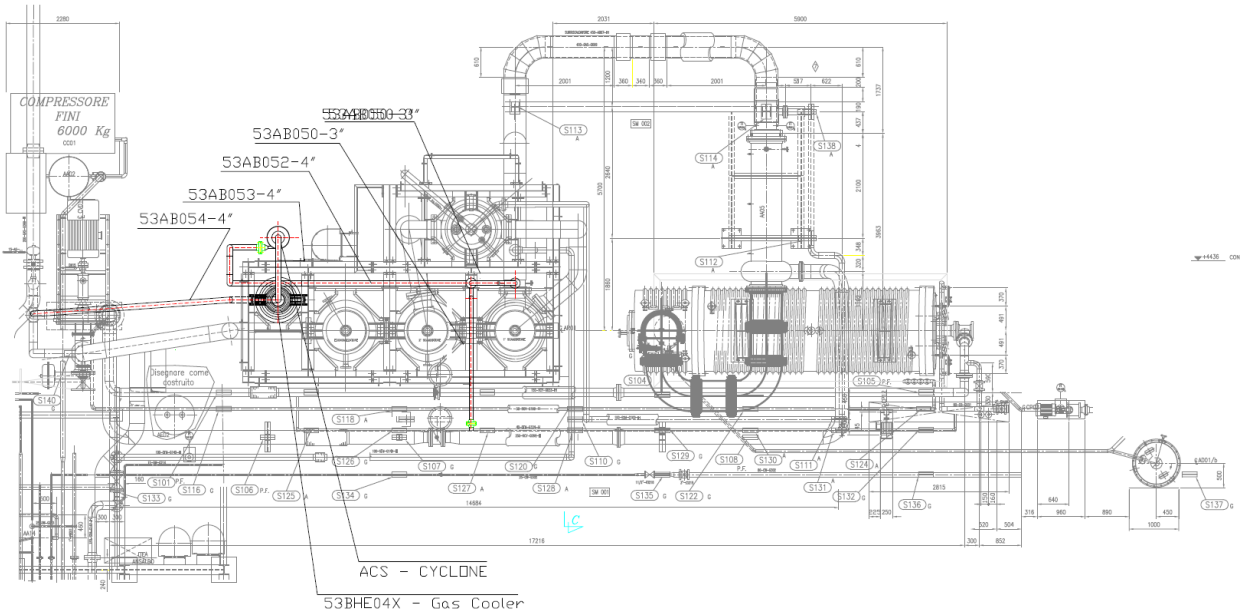

Figure 55. Proposed Facility Modification: Top View

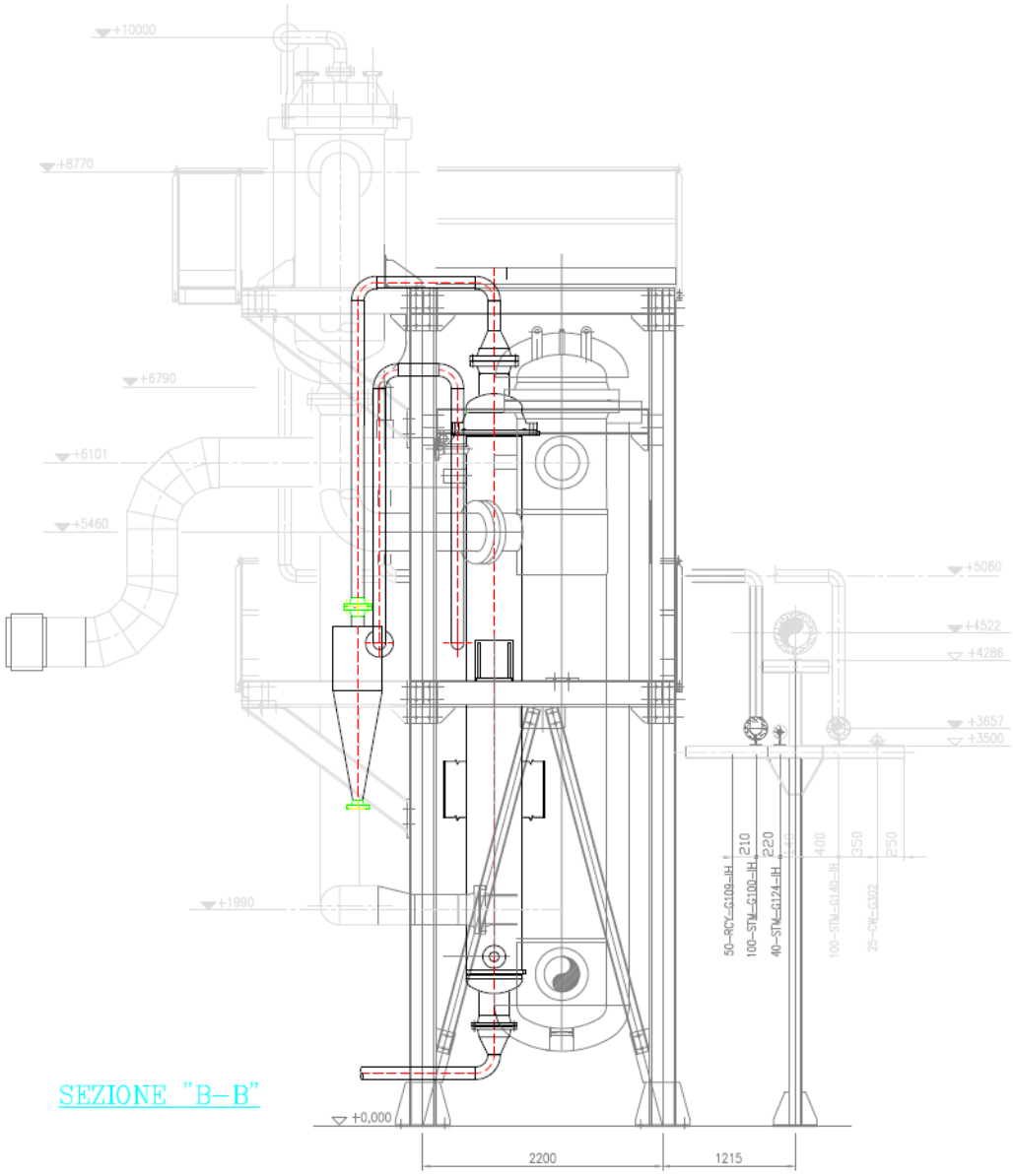

Figure 56. Proposed Facility Modification: Side View

5. REFERENCES

[1] I. G. Wright and J. Stringer, "Erosion and Corrosion Considerations for PFBC Gas Turbine Expanders," in International Gas Turbine Conference and Exhibit, Dusseldorf, West Germany, 1986.

[2] R. Parker and C. Seymour, "High-Temperature and High-Pressure Particulate Control Requirements," U.S. Environmental Protection Agency: Office of Research and Development, Washington D.C., 1977.

[3] M. First, J. B. Graham, R. Warren, G. Butler, and C. Walworth, "Test of "Fiberfrax" Ceramic Fibers for High Temperature Gas Filtration," Journal of the Air Pollution Control Association, vol. 6, no. 2, pp. 61-69, 1956.

[4] "SOx-NOx-Rox Box Flue Gas Cleanup Demonstration Project: Project Fact Sheet," 2003. [Online]. Available: https://www.netl.doe.gov/File%20Library/Research/Coal/major%20demonstrations/cctdp/Round2/snrb.pdf.

[5] Duffy, Robert J.; et al.; General Electric Company, Integral Engine Inlet Particle Separator, vol. 2, Cincinnati, Ohio: National Technical Information Service, August 1975.

[6] Rohsenow and Hartnett, Handbook of Heat Transfer, New York: McGraw-Hill, 1973.

[7] R. S. Wysk and L. A. Smolensky, "Novel Particulate Control Device for Industrial Gas Cleaning," Filtration and Separation, pp. 29-31, 1993.

[8] R. L. Salcedo and M. J. Pinho, "Pilot- and Industrial-Scale Experimental Investigation of Numerically Optimized Cyclones," Ind. Eng. Chem. Res., vol. 42, pp. 145-154, 2003.

[9] W. A. S. Zhao and M. B. Mujundar Ray, "Collection Efficiencies of Various Designs of Post Cyclone," Can. J. Chem. Eng., vol. 79, p. 708, 2001.

[10] J. Youngmin, T. Chi and B. R. Madhumita, "Development of a Post Cyclone to Improve the Efficiency of Reverse Flow Cyclones," Powder Technology, vol. 113, pp. 97-108, 2000.

[11] S. Sepehr, S. Mansoor, E. Mansooreh and F. Raheleh, "Improving the Removal Efficiency of Cyclones by Recycle Steam," Chem. Eng. Technol., vol. 29, no. No. 10, pp. 1242-1246, 2006.

[12] R. Salcedo, A. Fonseca, V. Chibante and G. Candido, "Fine Particle Capture in Biomass Boilers with Recirculating Gas Cyclones: Theory and Practice," Powder Tech. vol. 172, p. 89, 2007.

[13] G. Ramachandran, D. Leith, J. Dirgo and H. Feldman, "Cyclone Optimization based on a New Empirical Model for Pressure Drop," Aerosol Sci. Technol., vol. 15, pp. 135-148, 1991.

[14] R. Salcedo and M. Candido, "Global Optimization of Reverse-Flow Gas Cyclones: Application to Small-Scale Cyclone Design," Sep. Sci. Technol. vol. 36, pp. 2707-2731, 2001.

[15] H. Mothes and F. Loffler, "Prediction of Particle Removal in Cyclone Separators," Int. Chem. Eng, vol. 28, p. 231, 1998.